Improving diabetes care

SMPE/e nr 2008-020
June 12. 2008

TU/e

Appendices
Improving diabetes care:The development of a diabetes simulator

Ir. Ilham Saadane

Eindhoven, april 2008

/school of medical physics and engineering eindhoven

Appendices part of report:
SMPE/e nr: 2008-020
June 12, 2008

CIP-DATA LIBRARY TECHNISCHE UNIVERSITEIT EINDHOVEN

Saadane, Ilham

Improving diabetes care : the development of a diabetes simulator / by Ilham Saadane. - Eindhoven : Technische Universiteit Eindhoven, 2008. – (School of Medical Physics and Engineering Eindhoven : project reports ; 2008/002. – ISSN 1876-262X)
ISBN 978-90-386-1300-0
NUR 954
Keywords: Simulation / Diabetes / Education / Glucose-insulin model

Improving diabetes care: The development of a diabetes simulator

Appendices

Ir. Ilham Saadane

Appendices to the clinical project report of
The School of Medical Physics and Engineering Eindhoven

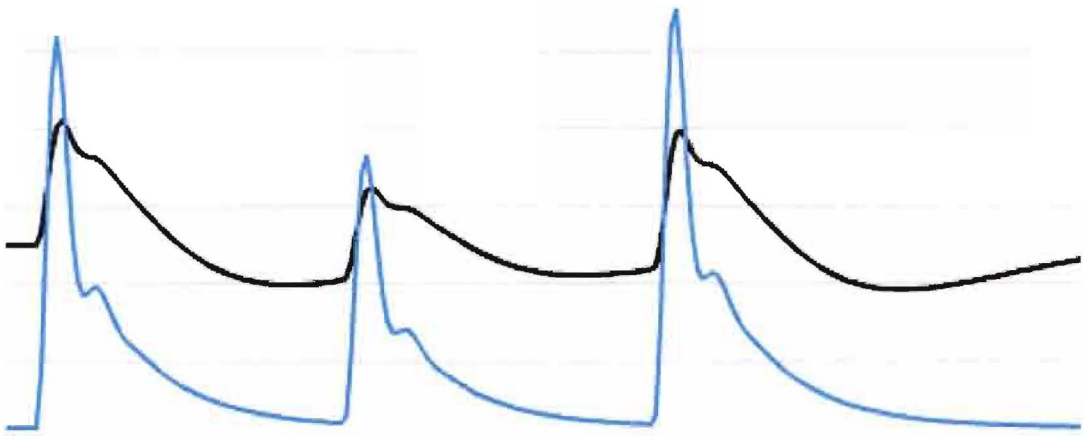

April, 2008

Supervised by:
Prof. F.N. van de Vosse
Dr. ir. E. Motoasca
Dr. ir. I.M.M. Lammerts
Dr. ir. C. van Pul
Dr. H.R. Haak

Contents

Appendix A: Pathophysiology of diabetes **5**
1. Diabetes 5
2. The physiology of glucose homeostasis 5
3. Diabetes management, complications and therapy 10
4. Diabetes education 14
5. Glucose monitoring 14

Appendix B: The glucose-insulin model **17**
1. Introduction 17
2. The classical minimal model of Bergman 18
3. The model of the gut 19
4. The β-cell secretion model 20
5. The subcutaneous insulin injection model 23
6. The renal glucose secretion model 23
7. Model equations 24

Appendix C: Initial model parameters **25**
1. Parameters 25
2. Initial conditions 28

Appendix D: Simulation of the glucose-insulin model **29**

Appendix E: Model performance **31**
1. Results for a healthy subject with initial parameters 31
2. Results with estimated parameters 33
3. Discussion 38
4. Conclusion 40

Appendix F: Parameter estimation using CGMS data **43**
1. Model equations 43
2. CGMS data 43
3. Parameter estimation 44
4. Discussion 46

Appendix G: The user interface of the simulator **47**

Bibliography **51**

Appendix A: Pathophysiology of diabetes

1. Diabetes

The prevalence of diabetes is rising all over the world. There are an estimated of 120 million people with diabetes world-wide. This number is predicted to increase, in both developed and developing countries to around 300 million by 2025. Diabetes is a serious and life-threatening condition, which is extremely costly [1].

There are different categories of diabetes mellitus (DM), of which the dominant primary one exists in two different forms, type I and type II diabetes. Type I diabetes, also known as insulin-dependent diabetes mellitus (IDDM). It is caused by an autoimmune disease and is characterized by a complete insulin deficiency due to the destruction of the beta cells producing the hormone insulin. Type II DM is much more common than type I DM, constituting about 90% of all cases of DM . In Type II diabetes, enough insulin may be available but, due to insulin resistance of the target organs, blood glucose regulation is perturbed [2].

A fasting blood glucose level of greater than or equal to 7.0 mmol/L, on at least two occasions, is diagnostic for diabetes. This test should be performed after an eight hour fast. Normal fasting glucose levels are less than 6.1 mmol/L, and normal two-hour postprandial (after a meal) glucoses are less than 7.8 mmol/L. Symptoms of hyperglycemia (e.g., polyuria[1], polydipsia[2], polyphagia[3], unexplained weight loss) with a casual blood glucose level of greater than or equal to 11.1 mmol/L also are sufficient to diagnose diabetes [2].

2. The physiology of glucose homeostasis

Energy requirements are determined by age, sex, body and size composition and levels of physical activity. Energy is derived from the oxidation of carbohydrate, protein and fat. Body energy stores are filled after meals and mobilized during

[1] Polyuria is a condition characterized by the passage of large volumes of urine (at least 2.5 L over 24 hours in adults).
[2] Polydipsia is a medical symptom in which the patient ingests abnormally large amounts of fluids by mouth.
[3] Polyphagia is a medical sign meaning excessive hunger and abnormally large (poly-) intake of solids by mouth.

fasting. Glycogen[4] is mainly stored in skeletal muscle, while triglyceride is stored in fat and is the major reserve. During starvation, body proteins can also be mobilized to produce amino acids that are converted into glucose fuel [3].

a. Carbohydrate metabolism

Blood glucose levels are normally maintained within tight limits by balancing glucose entry to the blood stream and glucose uptake by peripheral tissues. Tight glucose control is important in ensuring a steady state supply of glucose to the brain. The glucose level depends on the rate of glucose entry into the circulation and its uptake by the tissues. Under basal condition, the rates of glucose entry and uptake is equal and the blood glucose concentration is stable [3].

After digesting a meal, glucose concentrations in the blood rise with a speed and height that depends on the nature of the meal. Complex carbohydrates cause a slow rise with a low peak, while simple carbohydrates result in a rapid rise with a high peak. The skeletal muscle and liver are the main tissues that regulate blood glucose by varying their rates of glucose production and uptake. When the glucose levels rise, they stimulate the pancreatic beta-cells to secrete insulin. This cause glucose uptake in the insulin-dependent tissues like skeletal and cardiac muscles and fat. The ability of insulin to stimulate the maximum capacity for glucose uptake in these tissues is mainly dependent on the glucose transporter GLUT-4. In non-insulin dependent tissues (such as the central nervous system and red blood cells), glucose uptake (non-insulin-mediated glucose uptake) increases as blood glucose levels rise, through a mass-action effect. Insulin has little effect on glucose transporters GLUT-1 and GLUT-4 which are present in brain and other non-insulin dependent tissues. Once the blood glucose concentration dips below its basal value (5 mmol/L), the pancreas is stimulated to release glucagon which acts on the liver to release glucose. The liver can produce glucose via glycogenolysis[5] and gluconeogenesis[6]. A brief schematic representation of carbohydrate metabolism is shown in figure A.1 [3].

---

[4] Glycogen is a polysaccharide of glucose which functions as the primary short term energy storage in animal cells.
[5] Gluconeogenesis is the production of 'new'glucose from pyruvate, lactate, glycerol, and glucogenic amino acids.
[6] Glycogenolysis in the liver produces only a limited amount of glucose which can rapidly mobilized for use by other tissues.

Carbohydrate metabolism is regulated by several hormones and by the sympathetic and parasympathetic divisions of the autonomic system. By suppressing gluconeogenesis and glycogenolysis in the liver, insulin (the principal hormone) lowers blood glucose levels. When gluconeogenesis and glycogenolysis decreases, the hepatic glucose output decreases which causes glucose uptake into peripheral tissues (mainly muscle and adipose tissue). Hepatic glucose production can be inhibited by low insulin concentrations (30-60 mU/L), while much higher insulin levels are required to stimulate peripheral glucose uptake. These processes are opposed by the counter-regulatory hormones. These are secreted all the time but are released under conditions of physiological 'stress', including hypoglycemia, when the immediate mobilization of glucose is needed to increase blood glucose levels to normal. Glucagon is the main hormone that increases glucose output from the liver. It rapidly stimulates hepatic glucogenolysis and glucose production and subsequently increases gluconeogenesis. Therefore, this hormone reverses hypoglycemia. Catecholamines, including both adrenaline and noradrenaline, also stimulate glyconeogenesis, glycogenolysis and hepatic glucose production. Cortisol enhances gluconeogenesis as well, but has little effect on glycogen breakdown [3].

Between meals, the blood glucose levels are mainly determined by hepatic glucose production and peripheral glucose uptake. After an overnight fast, hepatic glucose output is about 1.8-2.2 mg/min/kg body weight. As the delivery of glucose from the intestine decreases during the transition from the fed to fasting state, the blood glucose levels are maintained by a progressive increase in hepatic glucose production. This is also the case during exercise, in order to meet increased muscle glucose use and maintain normal glucose levels. Hepatic glucose production must however be promptly suppressed after glucose ingestion to limit the rise in plasma glucose. Whole-body glucose utilization is equal to glucose production (1.8-2.2 mg/min/kg) in the basal state [3].

After an oral glucose consumption, 25 to 50% of the glucose load is taken by the liver. Of the extra glucose taken up by the peripheral tissues (compared with the basal state), the muscle accounts for 80-85% and adipose tissues for 10-20%. The brain has an obligatory requirement for glucose. It consumes 80% of the glucose utilized at rest after an overnight fast. Glucose uptake by the brain is not regulated by insulin or changes in blood flow, as it is in other tissues. Therefore, cerebral function is critically dependent upon maintaining blood glucose concentrations

within relatively narrow limits. Blood cells account for about 20% of total glucose requirements, and the renal medulla for most of the remainder [3].

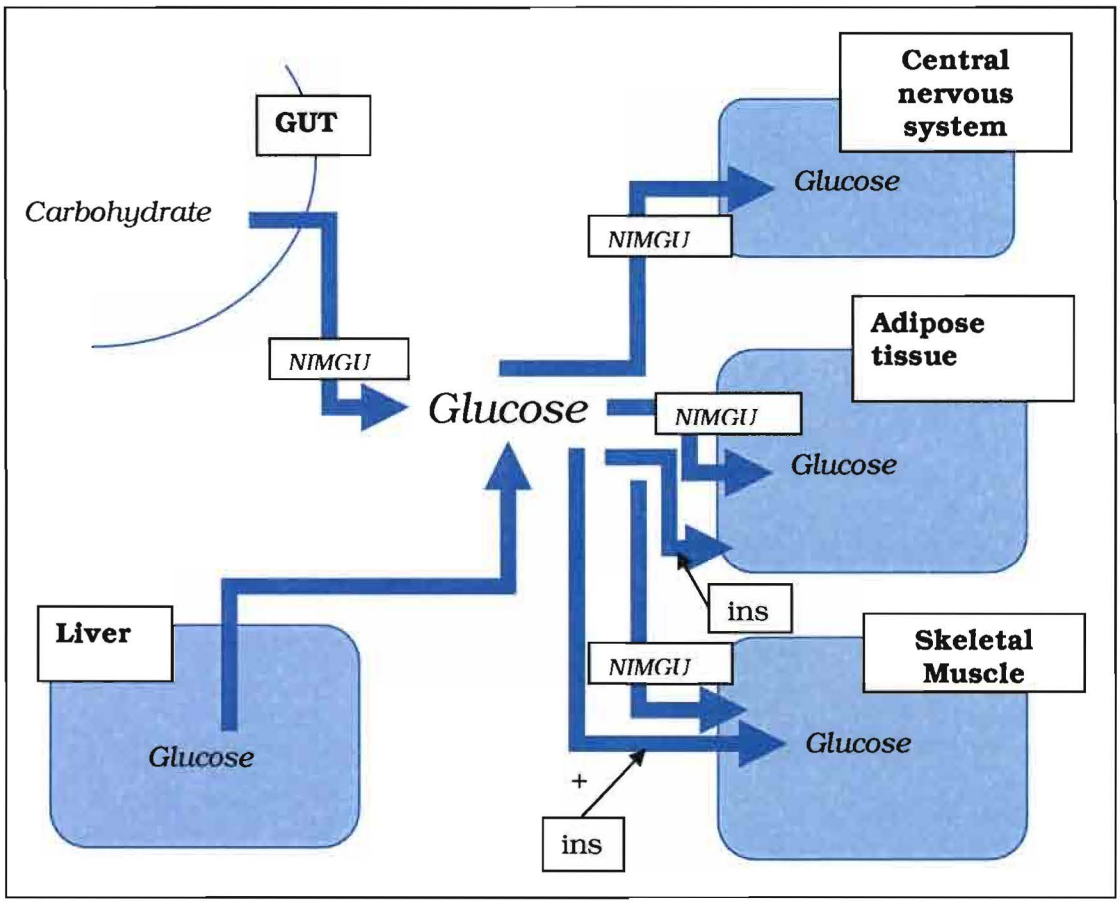

Figure A.1: Overview of carbohydrate metabolism [3]. Ins: insulin, NIMGU: non-insulin-mediated glucose uptake.

b. Fat and protein metabolism

The liver and adipocytes synthesize triglyceride from non-esterified fatty acids (NEFA) and glycerol-3-phosphate that is derived from glucose. Insulin stimulates lipogenesis by increasing glucose uptake into adipocytes via GLUT-4 and by inhibiting triglyceride breakdown (lipolysis) [3].

Protein production, which is around 200-300 gram per day, exceeds normal protein intake (70-100 g/day). Amino acids that are released from endogenous proteins are important in resynthesizing body proteins and producing glucose [3].

c. The effect of insulin

Insulin is a hormone that is secreted by the pancreatic beta-cells. These secrete about 40-50 units of insulin per day in normal adults. The basal concentration of insulin in the blood of fasting humans is on average 10 μU/ml (0.4 ng/ml or 61 pmol/L). Basal insulin secretion is the amount of insulin that is secreted in the absence of exogenous stimuli (in the fasting state). Insulin rarely rises above 100 μU/ml after standard meals. The peripheral insulin concentration begins to rise 8-10 minutes after ingestion of food and reaches a peak concentration in peripheral blood by 30-45 minutes. Consequently, postprandial plasma glucose concentration declines rapidly, which returns to baseline values by 90-120 minutes [4].

Stimulated insulin secretion, which occurs in response to exogenous stimuli, is the response of the beta-cell to ingested food. Glucose is the most potent stimulant of insulin release. When the glucose concentration in the system is increased suddenly, an initial short-lived burst of insulin secretion occurs, the early phase. If the glucose concentration is held at this level, the insulin release gradually falls off and then begins to rise again to a steady state level, the second phase. In the early phase, insulin is produced in a rapid burst, while in the second phase there is a less intense longer release lasting as long as blood glucose levels remain above basal levels. The first phase is important in priming the liver and muscles (insulin target tissues) so that they can respond to insulin. Persistent levels of high glucose stimulation (> 24 hours in vivo) results in a reversible desensitization of the beta-cell response to glucose but not to other stimuli [4].

Insulin's major function is to promote storage of ingested nutrients. Although insulin directly or indirectly affects the function of almost every tissue in the body, we will focus here on the effects of insulin on the three major tissues: liver, muscle and adipose tissue [3].

The liver is the first major organ that is reached by insulin via the bloodstream. Insulin promotes glycogen synthesis and storage at the same time it inhibits glycogen breakdown. The liver has a maximum storage capacity of 100-110 g of glycogen, or approximately 440 kcal of energy. Insulin also increases both protein and triglyceride synthesis and VLDL (very low density lipoprotein) formation by the liver. Next to that, it inhibits gluconeogenesis and promotes glycolysis.

Furthermore, insulin inhibits hepatic glycogenolysis, ketogensis and gluconeogenesis [3].

Insulin promotes protein synthesis in the muscle. It also promotes glycogen synthesis to replace glycogen stores expended by muscle activity. In the muscle tissue of a 70-kg man, approximately 500-600 g of glycogen is stored. However, it cannot be used as a source of blood glucose because of the lack of 6-phosphatase in the muscle, except by indirectly supplying the liver with lactate for conversion to glucose [3].

The most efficient means of storing energy is fat (in the form of triglyceride). It provides 9 kcal per gram of stored substrate (4 kcal/g is generally provided by protein or carbohydrate). The energy content of adipose tissue in the typical 70-kg man is about 100.000 kcal. Insulin acts to promote triglyceride storage in adipocytes by inducing the production of lipoprotein lipase which leads to hydrolysis of triglycerides from circulating lipoproteins , increasing glucose transport into fat cells and by inhibiting intracellular lipolysis of stored triglyceride by inhibiting intracellular lipase [3].

3. Diabetes management, complications and therapy

Diabetes is currently a chronic disease without a cure. The medical emphasis is on controlling and avoiding possible short- and long-term diabetes complications. In order to avoid these complications, DM patients should control their blood glucose. This can be achieved by combining diet, exercise and medication (oral diabetic drugs and/or insulin)[2] .
Chronic elevation of blood glucose will eventually lead to tissue damage. Whilst tissue damage can be found in many organs, it is the kidneys (nephropathy), eyes (retinopathy), peripheral nerves (neuropathy) and vascular tree, which manifest the most significant and sometimes fatal diabetic complications, figure A.3 [2].

Oral diabetes medications help control blood glucose levels in people who still produce insulin (the majority of people with type II DM). Several of these diabetes medicines are used in combination to achieve optimal blood glucose control. People with type I DM usually do not (or very little) produce insulin. For this group patients, insulin is required to control their blood glucose. In time, people with type

II DM develop beta-cell failure. This means that beta-cells in the pancreas that produce insulin no longer are able to secrete this hormone in response to high blood glucose levels. Therefore, type II DM patients often require insulin injections too, either in combination with their oral medications or alone .

The goal of diabetes therapy is tight glycaemic control, which delays the development of short-term complication such as hypoglycaemia [7] and hyperglycaemia [8] and long-term complications such as microvascular diseases. Glucose homeostasis results from the regulated balance among, glucose ingestion, hepatic glucose release, and skeletal muscle and adipose tissue glucose uptake and disposal. Pharmacologic treatment of diabetes patients targets all these components. There are several categories of oral diabetes medications. Different types and the way they work are listed in table A.1 [5].

[7] Hypoglycaemia is a pathologic state caused by a lower than normal level of glucose in the blood.

[8] Hyperglycaemia is a condition in which an excessive amount of glucose circulates in the blood.

Table A.1: Oral diabetes medication [5]

Type	How it works
Sulfonylureas	Lower the blood glucose by stimulating the pancreas to release more insulin. This medication is ineffective in type-1 diabetes because of β-cell destruction in this patient group.
Biguanides	Reduce hepatic glucose output and increase insulin-stimulated glucose uptake in skeletal muscle and adipocytes.
Thiazolidinediones	Reduce insulin resistance in skeletal muscle
Alpha-glucosidase inhibitors	Delay the intestinal absorption of carbohydrates through inhibition of the brush-border enzymes that hydrolyze polysaccharides to glucose.
Dipeptidyl peptidase-4 inhibitors	Increase Incretin levels which inhibit glucagon release, increase insulin secretion and decrease gastric emptying.

There are several types of insulin. The different types that are used in The Netherlands are classified below and in table A.2.

- Rapid-acting (Humalog®, NovoRapid® and Apidra®)
- Short-acting (Humuline® Regular, Actrapid®, Insuman® Rapid and Insuman® Infusat)
- Intermediate-acting (Humuline® NPH, Insulatard® and Insuman® Basal)
- Long-acting (Lantus® and Levemir®)
- Mix insulin (Humuline® 20/80, Humuline® 30/70, Mixtard® 50, Insuman® Comb 15, Insuman® Comb 25 and Insuman® Comb 50)

Insulin is ineffective when taken orally, and must therefore be given by other routes. It is taken as subcutaneous injections (into the layer of fat under the skin) by single-use syringes with needles, an insulin pump, or by repeated-use insulin pens with needles.

Table A.2: Pharmacokinetics of most commonly used insulin preparations

Insulin type	Onset of action	Time to peak effect	Duration of action
Rapid-acting	5 to 15 min	45 to 75 min	2 to 4 h
Short-acting	About 30 min	2 to 4 h	5 to 8 h
Intermediate-acting	About 2 h	6 to 10 h	18 to 28 h
Long-acting	About 2 h	No peak	20 to >24 h

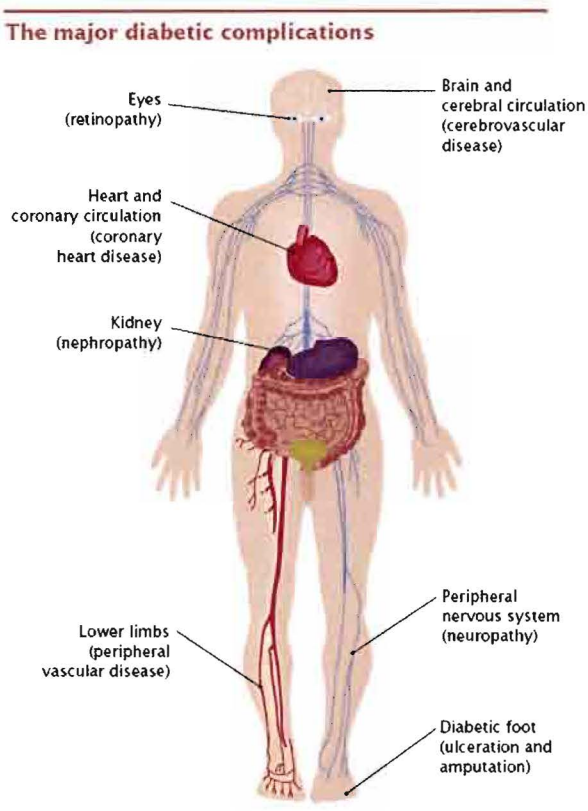

Figure A.3: Diabetes complications

4. Diabetes education

DM patients play an important role in determining their health status. Diabetes self-management is among the most difficult of all chronic illness self-management regimens. These patients must identify symptoms of emergencies (such as severe hypoglycemia), adhere to often complex medication schedules and modify their lifestyle such as their diet and physical activity. Therefore, many patients have difficulty in managing their disease [2] .

The goal of diabetes self-management education is to support the efforts of people with diabetes to: understand the nature of their illness and its treatment, identify emerging health problems in early reversible stages, adhere to self-care practices and make needed changes in their lifestyle.
Diabetes education programs range from one-on-one counseling to group sessions led by a clinician. Self-management educators can play an important role in empowering people with diabetes to become active participants in identifying self-care goals and overcoming barriers to their achievement [2].

5. Glucose monitoring

a. Self-monitoring

Blood glucose self-monitoring is very important in diabetes care as it may improve glycaemic control in DM patients. For this purpose, DM patients use glucose meters that are based on chemical test strips (figure A.4). These meters use a relatively small drop of blood (taken from the fingertip) that is placed on a disposable test strip. This strip interfaces with a digital meter that measures the level of blood glucose within several seconds.

Figure A.4: A glucose meter that is based on chemical test strips

b. HbA1c

Glycosylated hemoglobin (HbA1c) testing provides an index of average blood glucose levels over the prior two to three months. This testing method is used to assess long-term glycemic control.

Improved glycemic control is associated with preventing or delaying the progression of microvascular complications in diabetes. Hemoglobin formed in new red blood cells enters the circulation without any glucose attached. However, red cells are freely permeable to glucose. As a result, glucose becomes irreversibly attached to hemoglobin at a rate dependent upon the prevailing blood glucose. Several million red cells are destroyed every day, while an equal number of new ones are formed. Thus, the average amount of HbA1c changes in a dynamic way and reflects the mean blood glucose concentration over the previous two to three months.

c. Continuous monitoring

A continuous blood glucose monitor determines blood glucose levels on a continuous basis (every few minutes) for a few days (usually 3 days). A typical system consists of a disposable glucose sensor placed just under the skin, a link from the sensor to a non-implanted transmitter which communicates to a radio receiver, an electronic receiver (or insulin pump) that displays blood glucose levels (figure A.5). Continuous blood glucose monitors measure the glucose level of interstitial fluid. Therefore, calibration with a "finger stick" blood glucose measurement (2 to 4 times a day) is required. Glucose levels in interstitial fluid lag temporally (about 5 minutes) behind blood glucose values. Continuous monitoring allows examination of how the blood glucose level reacts to food, insulin, exercise, and other factors. Monitoring during periods when blood glucose levels are not typically checked (e.g. overnight) can help to identify problems in insulin dosing. A continuous monitor may also provide alarms to alert patients of hyperglycemia or hypoglycemia so that a patient can take corrective action(s) even in cases where they do not feel symptoms.

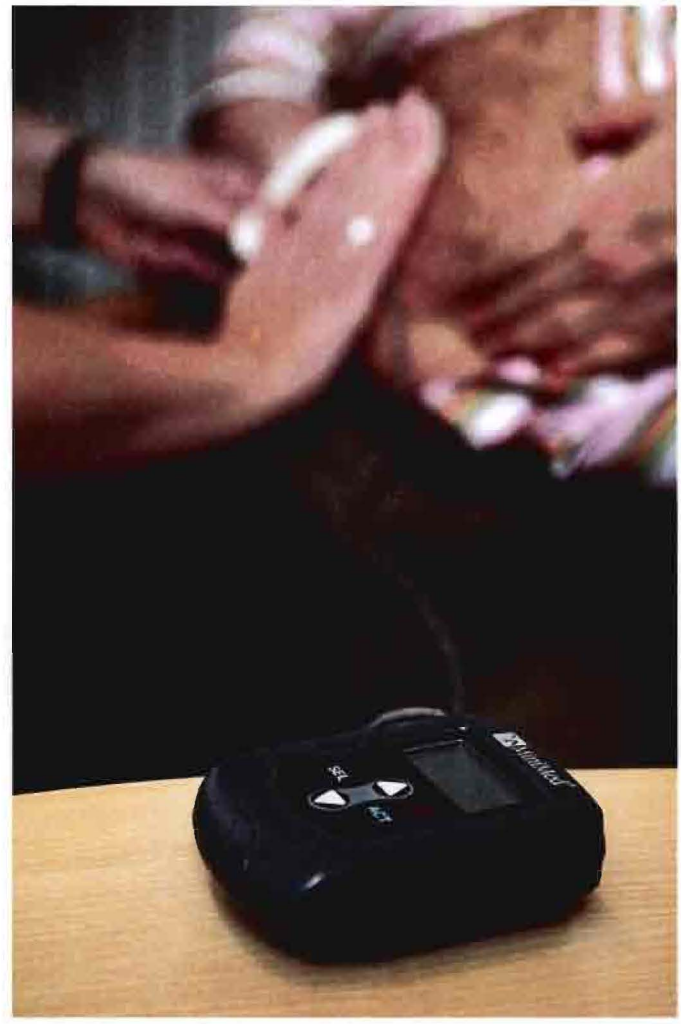

Figure A.5: Continuous Glucose Monitoring System (CGMS)

Appendix B: The glucose-insulin model

1. Introduction

This document describes a model of glucose-insulin interaction. This model was first developed by Bergman and colleagues [6] and describes glucose and insulin kinetics in healthy subjects. This model was developed to quantify insulin sensitivity from an intravenous glucose tolerance test (IVGTT). During an IVGTT, a known glucose concentration is injected into the blood plasma. The glucose and insulin concentration in blood plasma are then measured in time. The minimal model of Bergman is used to estimate parameters that are used to calculate an insulin sensitivity parameter (S_I). As this model doesn't contain a model of β-cell secretion, a model of subcutaneous insulin injection, a renal excretion model and a model of the gut, we added the β-cell secretion model of Steil [7], the gut model of Natalucci [8], the renal excretion model of Lehmann [9] and the injection insulin model of Berger & Rodbard [10]. A schematic representation of the complete model is represented in figure B.1.

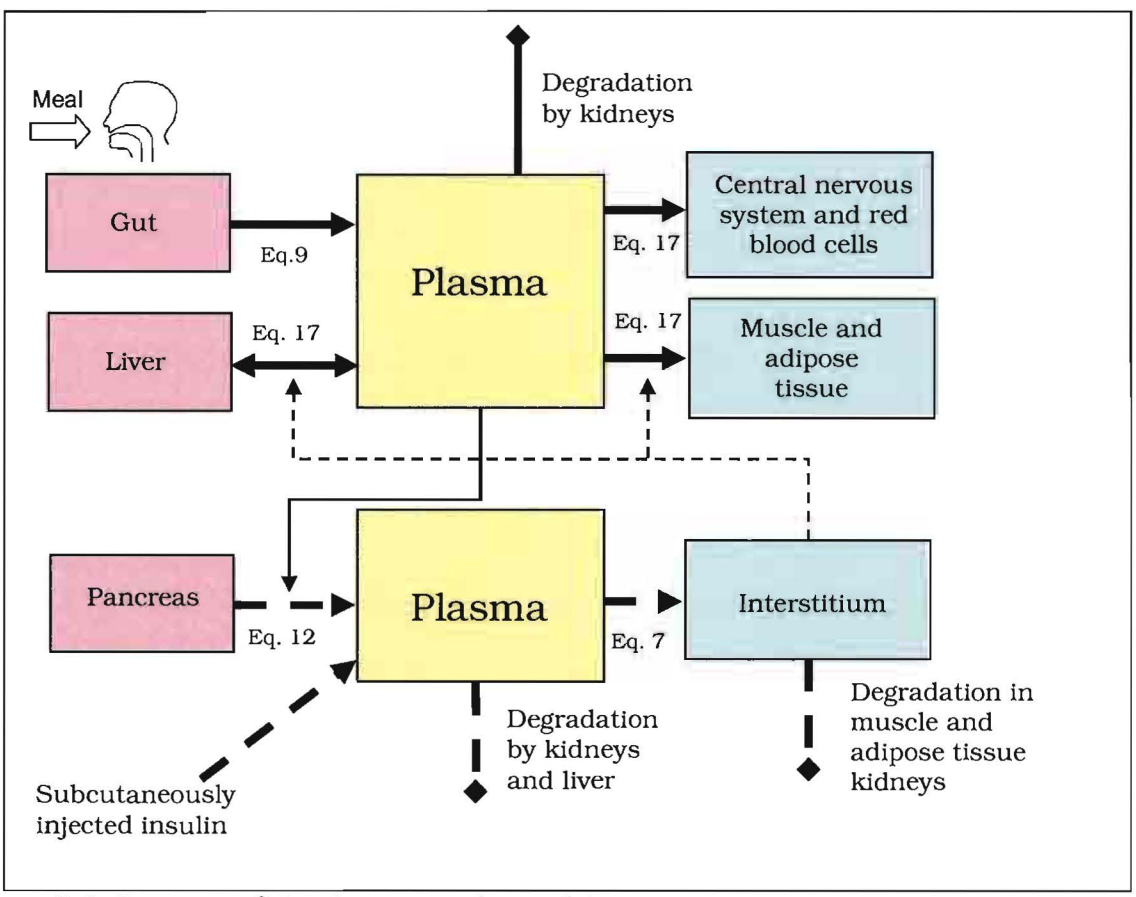

Figure B.1: Structure of the glucose-insulin model.

Glucose flow: ➡ , Glucose influence: ⟶ , Glucose degradation: ➡◆
Insulin flow ➡ , Insulin influence - - -▸ , Insulin degradation: ▬◆

2. The classical minimal model of Bergman

The classical model of Bergman [6] contains one plasma glucose compartment, one plasma insulin compartment and one remote compartment for insulin. Insulin concentration does not affect glucose dynamics directly, but acts through a "remote compartment". This compartment is called "remote" because the effective insulin concentration is not directly measurable [11]. Physiologically, the remote insulin compartment can be regarded as the interstitium in muscle and adipose tissue. The effective insulin concentration in the remote compartment, I_{eff} (μU/ml), is represented by:

$$\frac{dI_{eff}}{dt} = k_2\left(I_p(t) - I_b\right) - k_3 I_{eff}(t) \tag{1}$$

Where I_b (μU/ml) represents the basal insulin concentration, I_p (μU/ml) represents the insulin concentration in plasma and k_2 and k_3 represent the fractional rate parameters for insulin transport into and elimination from the remote compartment, respectively.

The rate of change of glucose G (mmol/L) in the blood plasma is given by:

$$\frac{dG}{dt} = \frac{dG_L}{dt} - \frac{dG_t}{dt} \tag{2}$$

where : $\frac{dG_L}{dt}$ is the net rate of glucose production by the liver and $\frac{dG_t}{dt}$ is the rate of glucose utilization by other tissues.

$$\frac{dG_L}{dt} = B_0 - k_5 G(t) - k_6 I_{eff}(t) G(t) \tag{3}$$

And

$$\frac{dG_t}{dt} = R_{d0} + k_1 G(t) + k_4 I_{eff} G(t) \tag{4}$$

In equation 3, B_0 represents the rate of glucose production by the liver, while the rate of glucose uptake by the liver is assumed to be proportional to an insulin-independent component (k_5) and insulin-dependent component $k_6 I_{eff}(t)$. In equation 4, the rate of glucose utilization by other tissues is assumed to have a constant component R_{d0}, a component proportional to glucose concentration k_1 and a component sensitive to both glucose and effective insulin concentration $k_4 I_{eff}(t)$. Substituting equations (3) and (4) into (2), we obtain:

$$\frac{dG}{dt} = [B_0 - R_{d0}] - [k_5 + k_1]G(t) - [k_6 + k_4]I_{eff}(t)G(t) \qquad G(t_0) = G_0 \tag{5}$$

where G_0 (mmol/L) is the glucose concentration at the beginning (t_0)of the simulation.

Since I_{eff} is not measurable, a further reduction in parameters is achieved by the introduction of a new variable I_{rem} (1/min) that is proportional to I_{eff}:

$$I_{rem}(t) \equiv [k_6 + k_4]I_{eff}(t) \tag{6}$$

By substituting equation (6) into equations (1) and (5), we obtain:

$$\frac{dI_{rem}}{dt} = -p_2 I_{rem}(t) + p_3\left(I_p(t) - I_b\right) \qquad I_{rem}(t_0) = I_{rem0} \tag{7}$$

and

$$\frac{dG}{dt} = -p_1 G(t) - I_{rem}(t)G(t) + p_1 G_b \qquad G(t_0) = G_0 \tag{8}$$

where $p_1 = k_1 + k_5$ [1/min], $p_2 = k_3$ [1/min], $p_3 = k_2(k_4 + k_6)$ [ml/μU/min²], G_b [mmol/L] is the basal glucose concentration in the blood plasma and $p_1 G_b = B_0 - R_{do}$.

3. The model of the gut

Glucose enters the plasma compartment not only via hepatic (liver) glucose production but also via intestinal absorption. This part was not modeled in Bergman's model [6]. Therefore, we will couple the classical minimal model to the model of the gut from Natalucci [8]. Glucose absorption from the gut is described by equation:

$$\frac{dG_{gut}(t)}{dt} = D_G k \beta e^{(-kt)^\beta} - k_{abs} G_{gut}(t) \qquad G_{gut}(t_0) = G_{gut0} \tag{9}$$

where, G_{gut} (mmol) is the mass of glucose in the gut, D_G (mmol) represents the amount of ingested glucose, k [min] is the time constant of gastric emptying, β is the power of the curve, t (min) is the independent model variable, G_{gut0} (mmol) is the glucose concentration in the gut at t_0 and k_{abs} (1/min) is the rate constant of glucose absorption from the gut into blood plasma. By adding the model of the gut, we obtain:

$$\frac{dG}{dt} = -p_1 G(t) - I_{rem}(t)G(t) + p_1 G_b + \frac{k_{abs} G_{gut}}{V_G} \qquad G(t_0) = G_0 \tag{10}$$

Where: V_G (l/kg) is the volume of glucose distribution per kg body weight.

4. The β-cell secretion model

The pancreas β-cell has a biphasic response to glucose variations. The "first" and "second" β-cell phase response are clearly seen during hyperglycemic clamps, in which the amount of glucose necessary to compensate for an increased insulin level without causing hypoglycemia is measured, see figure B.2. The first-phase insulin concentration peak and the rate of increase of second phase insulin (slope) are both proportional to the increment in plasma glucose, see figure B.2b. Defects in first-phase insulin release have been linked with the etiology of type 2 diabetes [12] and improvements in this response has been linked to improvements in glucose tolerance [13], [14]. Since glucose uptake is proportional to glucose concentration times insulin effect, an early insulin response results in less total insulin needed to yield a similar area under the glucose excursion [11]. It is thought that first-phase insulin results in an early suppression of hepatic glucose output.

The β-cells' biphasic insulin response can be compared to the response of a proportional (P), integral (I), and derivative controller (D), PID-controller [15]. The proportional component reacts to the difference between plasma glucose and basal glucose, the integral component reacts to persistent hyper- or hypoglycaemia and the derivative component reacts to the rate of change in plasma glucose. Hence, the integrator and derivative components produce the slow second-phase rise and rapid first-phase rise seen during hyperglycemic clamps, figure B.3.
Insulin delivery (I_D) by the pancreas as predicted by a PID-controller is described by:

$$
\begin{aligned}
&I_D(t) = P(t) + I(t) + D(t)\ ; && I_D(t) \geq 0 \\
&P(t) = K_p\left(G(t) - G_b\right) && \\
&I(t) = \frac{K_P}{T_I}\int_{t_0}^{t}\left(G(t) - G_b\right)dt; && I(t_0) = I_{DB} \qquad (11) \\
&D(t) = K_p T_D \frac{dG(t)}{dt} &&
\end{aligned}
$$

where the proportional gain K_p (units/h per mmol/l) determines the rate of insulin delivery in response to glucose above the basal level (G_B; mmol/l), T_I (integral time; min) determines the rate at which the underlying basal rate adapts, and T_D (derivative time; min) determines the relative amount of insulin delivered in response to the rate of change of glucose. The value of K_p is set in relation to the total daily dose (T_{DD}) of insulin as follows:

$$K_p = T_{DD} \times \frac{K_{p,reference}}{T_{DD,reference}}$$

A patient's T_{DD} depends on the function of the pancreas β-cells. With decreasing beta-cell function resulting in decreased insulin production, subjects with type 1 diabetes may require insulin. In general, type 1 diabetics generally require 0.5-1.0 units per kg of body weight per day of insulin. During the early stages of type 1 diabetes, patients will require less insulin injections because the β-cells are still producing some insulin; insulin requirements can be in the range of 0.1-0.6 units per kg per day. In our model the T_{DD} will be patient-specific. For healthy persons, the T_{DD} is set to 1 unit per kg of body weight.

The proportional component of the PID-controller increases insulin delivery when glucose is above target and reduces insulin delivery when glucose is below target level. When glucose is at target level, the P component provides no contribution. Thus, it does not contribute to the underlying basal requirement needed to maintain fasting glucose at target. The integration component is the only component to provide insulin when glucose is at target and stable and is comparable to basal insulin secretion. It adjusts upward when glucose is above target level, downward when glucose is below target level, and is unchanged when glucose is at target level. It ensures that target is always achieved when the system is at steady state. The derivative component increases insulin delivery when glucose is rising and decreases delivery when glucose is falling. This stabilizes the system in such a way that any change in plasma glucose is counteracted by a change in insulin delivery; regardless of the prevailing glucose level (it stops for example insulin delivery when glucose is falling, even if the glucose level is above target).

Insulin is secreted from the β-cell into plasma at a rate proportional to p_5 (1/ml) and is eliminated at a rate proportional to k_e (1/min). This process is described by the following equation:

$$\frac{dI_p}{dt} = p_5 I_D(t) - k_e I_p(t) \qquad I_p(t_0) = I_{p_0} \qquad (12)$$

where, I_p represents plasma insulin and I_{p0} is the insulin concentration in the blood plasma at t_0.

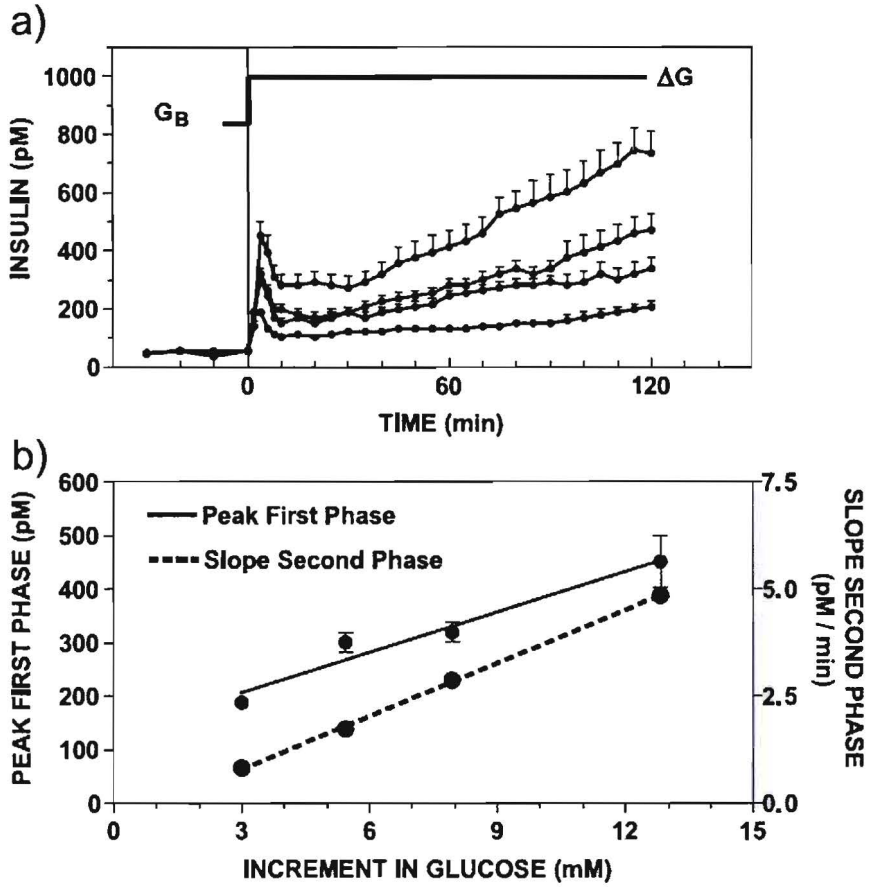

Figure B.2: (a) Plasma insulin concentrations during hyperglycemic clamps with increasing glucose levels. (b) First-phase response peak (left axis; solid line) and slope of second-phase (dashed line) versus increment in glucose [15].

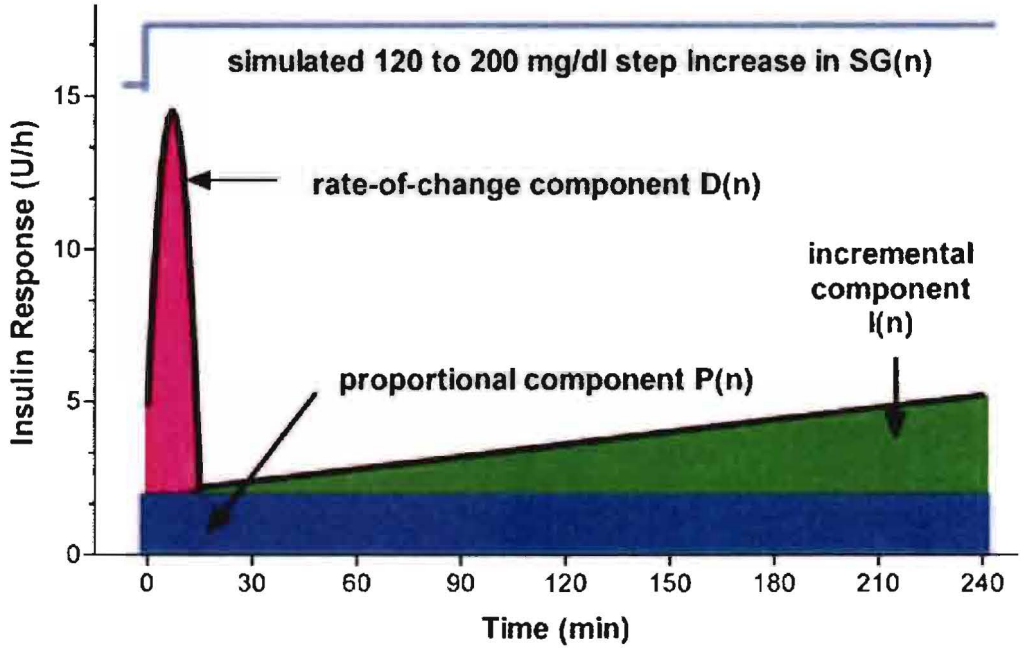

Figure B.3: Theoretical response of the PID algorithm to a hyperglycemic clamp. The response is shown for K_P=0.025 units/h per mg/dl, T_I=150 min and T_D=66 min [16].

5. The subcutaneous insulin injection model

When simulating blood glucose profiles in diabetes patients, the beta-cell secretion model will be modified or disconnected from the model as the beta-cell is not working properly/anymore in these patients. In this case, insulin will be injected subcutaneously (external input).

The pharmacokinetics of injected insulin absorption have been derived from Berger & Rodbard [10]. The rate of insulin absorption I_{inj} is modeled as follows:

$$I_{inj} = \frac{s\left(\frac{t}{T_{50}}\right)^{s} D_I}{t\left(1+\left(\frac{t}{T_{50}}\right)^{s}\right)^{2}} \tag{13}$$

where t is the time elapsed from the injection, T_{50} is the time at which 50% of the insulin dose, D_I, has been absorbed and *s* is an insulin specific parameter defining the insulin absorption pattern of the different types of insulin used in the model (short-, intermediate- and long-acting). T_{50} on dose is defined as:

$$T_{50}{}^{s} = aD_I + b \tag{14}$$

where a and b are also insulin specific parameters. The values of these parameters are given in table C.2.

By adding the subcutaneous insulin injection model, equation 12 will become:

$$\frac{dI_p}{dt} = p_5\left(I_D(t) + I_{inj}\right) - \mathrm{k_e} I_p(t) \qquad I_p(t_0) = I_{p_0} \tag{15}$$

6. The renal glucose secretion model

The function of the kidney is modeled in terms of renal threshold of glucose and creatinine clearance [9]. Glucose excretion from the model takes place above the renal threshold as a function of the creatinine clearance rate. The rate of renal glucose excretion G_{ren} is defined as follows:

$$\begin{cases} G_{ren} = G_{FR}\left(G - R_{TG}\right); & \mathrm{G} > \mathrm{R_{TG}} \\ G_{ren} = 0; & (\text{elsewhere}) \end{cases} \tag{16}$$

where G_{FR} is the glomerular filtration (creatinine clearance) rate. Default parameter values for R_{TG} and G_{FR} are set to 9 mmol/l and 100 ml/min respectively. The renal excretion of glucose is zero for blood glucose values below the renal threshold of glucose. By adding the renal glucose excretion model, equation 10 becomes:

$$\frac{dG}{dt} = -p_1 G(t) - I_{rem}(t) G(t) + p_1 G_b + \frac{k_{abs} G_{gut}}{V_G} - \frac{G_{ren}}{V_G} \qquad G(t_0) = G_0 \qquad (17)$$

7. Model equations

The differential equations that describe the glucose-insulin model are:

$$\frac{dG_{gut}(t)}{dt} = D_G k \beta e^{(-kt)^{\beta}} - k_{abs} G_{gut}(t) \qquad G_{gut}(t_0) = G_{gut0} \qquad (9)$$

$$\frac{dG}{dt} = -p_1 G(t) - I_{rem}(t) G(t) + p_1 G_b + \frac{k_{abs} G_{gut}}{V_G} - \frac{G_{ren}}{V_G} \qquad G(t_0) = G_0 \qquad (17)$$

$$\frac{dI_{rem}}{dt} = -p_2 I_{rem}(t) + p_3 \left(I_p(t) - I_b \right) \qquad I_{rem}(t_0) = I_{rem0} \qquad (7)$$

$$\frac{dI_p}{dt} = p_5 \left(I_D(t) + I_{inj} \right) - k_e I_p(t) \qquad I_p(t_0) = I_{p_0} \qquad (12)$$

These equations are implemented, along with the initial conditions, in Simulink®. A schematic representation of the Simulink® model is given in appendix D.

Appendix C: Initial model parameters

1. Parameters

The model parameters of Bergman et al. [17] were determined from a human study in which they performed an intravenous glucose tolerance test (IVGTT) in 18 subjects. The subjects were in good health and were not taking any medication that would alter carbohydrate metabolism. The subjects were divided in 4 groups lean (88-105% Ideal Body Weight) with good glucose tolerance, lean with low glucose tolerance, obese (130-206% IBW) with good tolerance and obese with low tolerance. For the development of our model, we considered the parameters p_1, p_2, p_3 and G_b of the first group "lean with good tolerance", see table C.1, as the basis of our model should behave like a healthy person.

Tabel C.1: Model parameters (Bergman, 1981)

Subjects	Sex	Ib [uU/ml]	Gb [mmol/l]	p1 [1/min]	p2 [1/min]	p3 [min-2/uU/ml]
1	M	17	5.22	2.96E-02	1.86E-02	6.51E-06
2	M	9	5.06	1.92E-02	2.62E-02	1.47E-05
3	M	15	4.72	3.74E-02	4.78E-02	8.73E-06
4	M	8	5.50	3.63E-02	8.10E-03	4.01E-06
5	M	9	5.17	4.64E-02	3.80E-03	3.61E-06
AVG		11.60	5.13	3.38E-02	2.09E-02	7.51E-06
STD		4.10	0.28	1.01E-02	1.74E-02	4.52E-06

In the study of Natalucci [8], nine nondiabetic subjects received an oral glucose tolerance test (OGTT). From the measured data, the parameter k_{abs} was derived and was used in our model. Parameters k and β were derived from the study of Schirra [18]. This study investigated in eight healthy male volunteers (age: 24-28 yrs; IBW=10%) the gastric emptying pattern of glucose. To develop a physiologically plausible parametric description of glucose gastric emptying Natalucci *et al* took the derivative of power exponential equation $f(t) = \exp(-kt)^{\beta}$ that Schirra *et al* used to fit the experimental gastric emptying curve (the amount of glucose retained in the stomach expressed as percentage of the total glucose ingested) observed during OGTT. The equation for gastric emptying R_{ge} is described as follows:

$$R_{ge}(t) = -D\frac{df}{dt} = Dk\beta\exp(-kt)^{\beta} \qquad (18)$$

The derivative df/dt was multiplied by the amount of glucose ingested, D, to express R_{ge} in mg/min. The minus sign indicates that R_{ge} enter the gut compartment.

Steil *et al* [7] evaluated two secretion models for their ability to describe plasma insulin dynamics during hyperglycaemic clamps in seven nondiabetic subjects (five men, two women; age: 48 ± 2 yrs; BMI=25.7 ± 0.8 kg/m²). We used the PID model, as described above, as it was the most suitable model.

Table C.2 gives descriptions and values for all the model parameters, which were taken from the literature [17], [8], [18],[7]and [10].

Table C.2: Model parameters

Parameter	Unit	Description	Value	Ref
G(t)	[mmol/l]	Plasma glucose	Calculated	
G_B	[mmol/l]	Basal glucose level	5.13 ± 0.28	[17]
G_0	[mmol/l]	Glucose concentration at t_0	Patient-specific	
$G_{gut}(t)$	[mmol]	Glucose concentration in the gut	Calculated	
$I_p(t)$	[μU/ml]	Plasma insulin	Calculated	
$I_{eff}(t)$	[μU/ml]	Effective insulin	Calculated	
$I_D(t)$	[μU/min]	Physiological insulin delivery	Calculated	
$I_{rem}(t)$	[1/min]	Variable proportional to I_{eff}	Calculated	
I_{p0}	[μU/ml]	Insulin concentration at t_0	Patient-specific	
k_1	[1/min]	Rate of insulin-independent glucose utilization by non-hepatic tissues	Not identifiable	
k_2	[1/min]	Fractional rate parameter for insulin transport into remote compartment	Not identifiable	
k_3	[1/min]	Fractional rate parameter for insulin transport from remote compartment	Not identifiable	
k_4	[1/μU/ml/min]	Rate of insulin-dependent glucose utilization by non-hepatic tissues	Not identifiable	
k_5	[1/min]	Rate of insulin-independent glucose uptake by the liver	Not identifiable	
k_6	[1/μU/ml/min]	Rate of insulin-dependent	Not identifiable	

		glucose uptake by the liver		
B_0	[mmol/l/min]	Rate of glucose production by the liver (constant component)	Not identifiable	
R_{d0}	[mmol/l/min]	Rate of glucose utilization by non-hepatic tissues (constant component)	Not identifiable	
p_1	[1/min]	$p_1 = k_1 + k_5$	$3.38 \pm 1.01 \cdot 10^{-2}$	[17]
p_2	[1/min]	$p_2 = k_3$	$2.09 \pm 1.74 \cdot 10^{-2}$	[17]
p_3	[ml/μU/min²]	$p_3 = k_2 (k_4 + k_6)$	$7.51 \pm 4.52 \cdot 10^{-6}$	[17]
p_5	[1/ml]	Insulin secretion rate from the beta-cell into the plasma	$p_5 = 1/V_I$	
$K_{p,reference}$	[μU/min per mmol/l]		0.675 [U/h per mg/dl]= $0.2 \cdot 10^6$ [μU/min per mmol/l]	[19]
$T_{DD,reference}$	[U/min]	Reference total daily dose	1 [U/kg body weight per day]= 0.0486 [U/min] (70 kg)	[19]
T_{DD}	[U/min]	Total daily dose	Variable between 0.5 and 1 U/kg per day	
K_p	[μU/min per mmol/l]	Rate of insulin secretion in response to glucose above basal		[19]
T_I	[min]	Ratio of proportional to integral release	98.8	[7]
T_D	[min]	Ratio of derivative to proportional release	37.6	[7]
I_{DB}	[μU/min]	Basal insulin delivery rate	0	[19]
D_G	[mmol]	Amount of glucose ingested	Variable	

k_{abs}	[1/min]	Rate of glucose absorption from the gut into blood plasma	$2.89 \cdot 10^{-2}$	[8]
k	[1/min]	Time constant of gastric emptying	0.014	[8]
β	dimensionless	Power of the exponential curve	1.23	[8]
V_G	[1]	Volume distribution for glucose per kg body weight	0.17 [l/kg]	[8]
V_I	[ml]	Volume distribution for insulin per kg body weight	$0.142 \cdot 10^3$ [ml/kg]	[9]
w	kg	Body weight	Patient specific	
k_e	[1/min]	Insulin elimination rate	0.09	[7]
I_{inj}	[μU/min]	Subcutaneously injected insulin	Calculated	[10]
T_{50}	[min]	Time at which 50% of the insulin dose has been absorbed	Calculated	[10]
s	dimensionless	Insulin preparation specific parameter	s(regular)= 2	[10]
a	[min/ μU]]	Insulin preparation specific parameter	a(regular)=0.05 [h/U]=(0.05x60) $\cdot 10^{-6}$ [min/ μU]	[10]
b	[min]	Insulin preparation specific parameter	b(regular)= 1.7 [h]=1.7x60=102 [min]	[10]
D_I	[μU]	Insulin dose		
G_{ren}	[mmol/l per ml/min]	Rate of renal glucose excretion	Calculated	
G_{FR}	[ml/min]	Glomerular filtration rate	100 ml/min (default)	[9]
R_{TG}	[mmol/l]	Renal threshold of glucose	9 mmol/l (default)	[9]

2. Initial conditions

In equation 15 and 17, G_0 and I_{p0}, the initial of glucose and insulin in blood plasma, depends on the carbohydrate consumptions and insulin injection (for insulin-dependant patients) the night/evening before the start of the simulation. So, these parameters are patient/scenario-specific. G_{gut0} and I_{p0} are set to zero as we assume that there is no glucose in the gut and no insulin in the plasma after night fasting.

Appendix D: Simulation of the glucose-insulin model

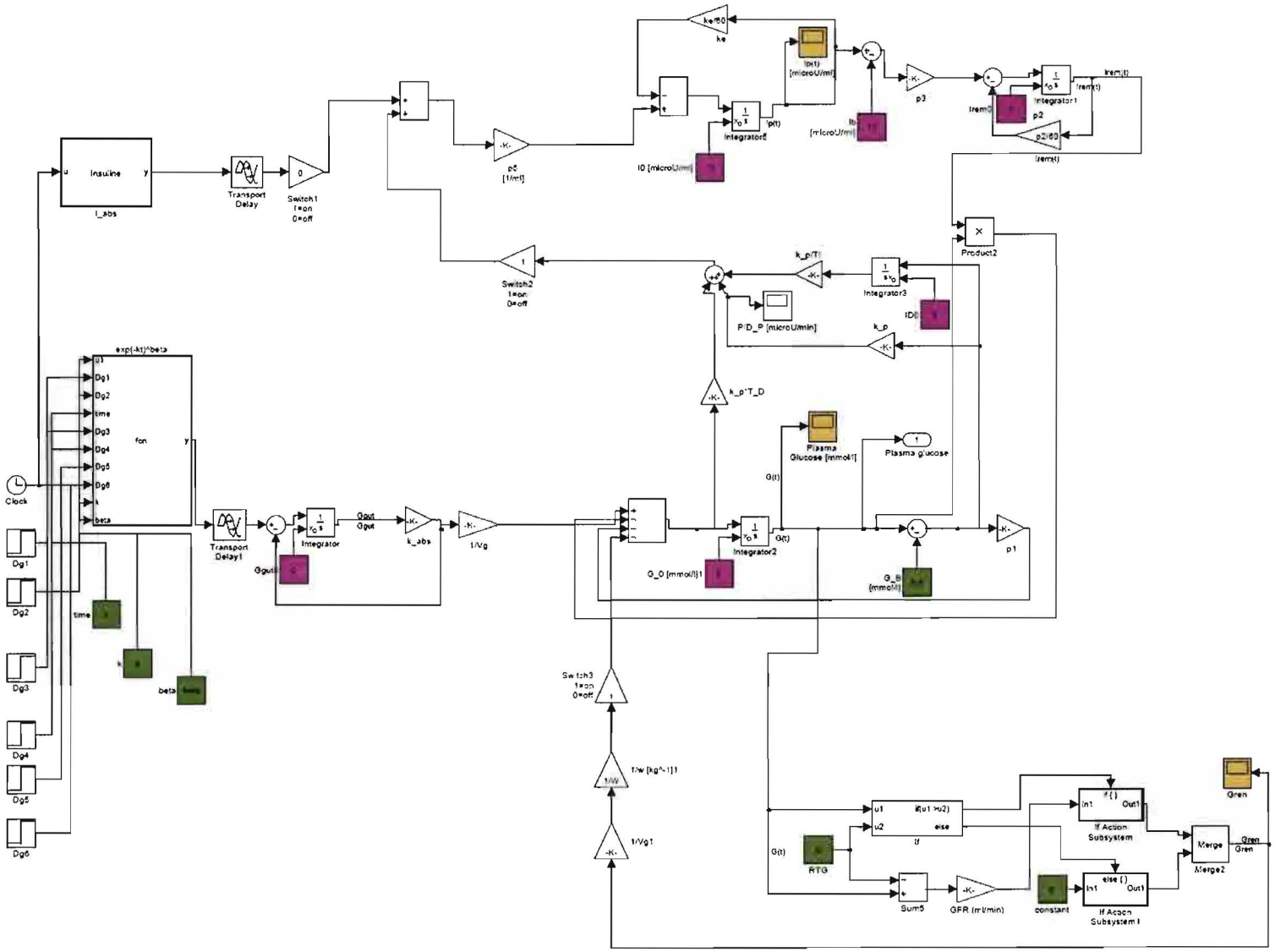

Appendix E: Model performance

1. Results for a healthy subject with initial parameters

Figure E.1 shows the glucose and insulin concentration time-courses of a 70 kg healthy subject, predicted by our model, before and after the consumption of 75 g glucose (solid line). Glucose was orally ingested at t=0 min.

a. Rate of glucose appearance into plasma

The rate of glucose appearance into plasma reaches its maximum (600 mg/min) 48 minutes after glucose consumption, figure E.1. Our results (red dots in figure E.2) are within the 95% confidence interval of the predicted rate of glucose appearance by Natalucci et al [8] where a maximum (between 400 and 700 mg/min) is reached at around 50 minutes, figure E.2.

b. Insulin delivered by the pancreas

Figure E.1 shows also the simulated response of the pancreas to the glucose input (plasma glucose trace in figure 3). Insulin delivery rate reaches its maximum of about 25 U/h at 12 minutes from glucose consumption. Our results are comparable to Steil [16]. The shape of the simulated pancreas response is slightly different from figure B.3 because the input in figure B.3 was a step function, whereas the input (for the Insulin delivery system) was the plasma glucose trace shown in figure E.1.

c. Insulin concentration in the plasma

The maximum insulin concentration in the plasma is around 350 μU/ml (figure 3). The insulin concentration in the plasma is not within the physiological range for a healthy human (up to 100 μU/ml), see appendix A. The predicted plasma insulin immediately begins to rise after ingestion of food and reaches a peak concentration by 18 minutes. This is not the case in vivo, where the insulin concentration begins to rise 8-10 minutes after ingestion of food and reaches a peak concentration by 30-45 minutes, see appendix A.

d. Glucose concentration in the plasma

Figure 3 shows that the predicted glucose concentration in the plasma is also within the normal range for a healthy person (4 to 8 mmol/L). However, the plasma glucose trace should be validated against measured glucose data.

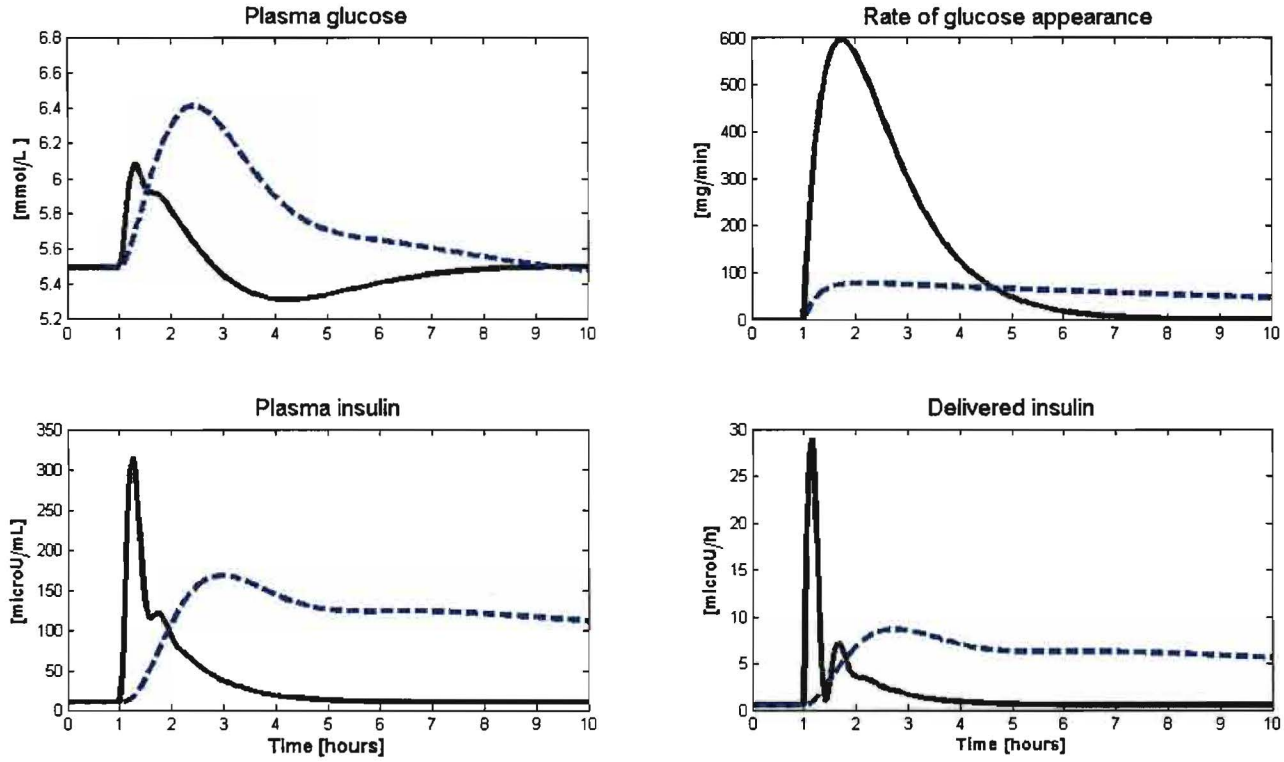

Figure E.1: Glucose and insulin concentrations predicted by the model using parameters from the literature (solid line) and estimated parameters (dashed line). These results are obtained for a 70 kg healthy person, where glucose was orally ingested at t=1 h (no exogenous insulin was injected). There is a difference between the simulated glucose and insulin profiles for literature parameters and estimated parameters. This difference is caused by the fact that the estimated parameters are fitted to the measured data

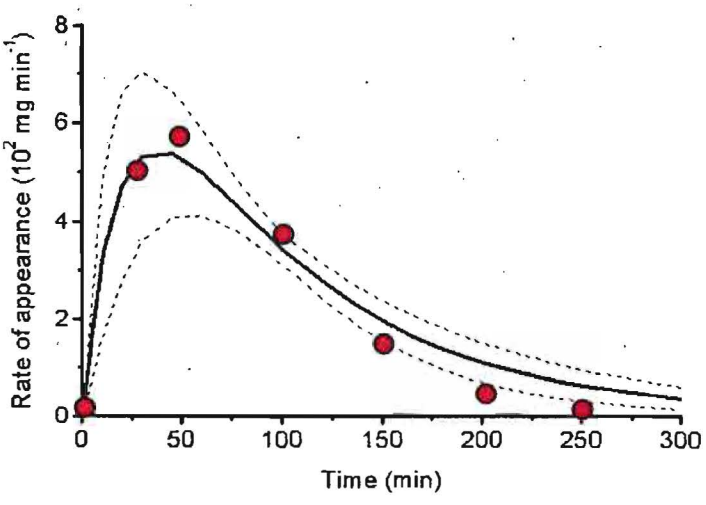

Figure E.2: Average (with 95% confidence interval) rate of glucose appearance into plasma predicted by the gut-model of Natalucci [8]. The parameters of the model are estimated from nine non-diabetic subjects that ingested a glucose load (75 g) at time t=0 min. For comparison, the figure also shows the predicted rate of glucose appearance by our model (the red dots), where the same input (D_G=75 g) is used (figure E.1).

2. Results with estimated parameters

In order to improve the results of our model we estimated the parameters of the model using a 17 hour Continuous Glucose Monitoring System (CGMS) data. These data were measured on 11 healthy normoglycaemic subjects (Age=59 ± 2 years; BMI=27.8 ± 1.4 kg/m^2). More information about the measurement procedure and the subjects is given in [20]. The Parameter Estimation toolbox of Simulink® was used to perform the estimation. Table E.1 shows the initial (from the literature) and estimated parameters. A detailed description of the estimation of the parameters is shown in appendix F.

Table E.1: Initial and estimated model parameters of a healthy person

Parameter	Initial	Estimated	Unit
Kp	200000	114060	μU/min per mmol/L
Td	40.0	0.003	min
Ti	100.0	199.95	min
beta	1.23	0.32	dimensionless
k	0.0140	0.0035	1/min
kabs	0.029	0.058	1/min
ke	0.090	0.085	1/min
p1	0.034	0.016	1/min
p2	0.021	0.019	1/min
p3	$7.5 \cdot 10^{-6}$	$0.57 \cdot 10^{-6}$	ml/μU/min^2

a. Results of a multiple meals simulation in a healthy person

We used the new estimated parameters to simulate multiple meals, with breakfast at 8 a.m. (129 g), a snack at 10.30 a.m. (28 g) and lunch at 12.30 a.m. (86 g). The results of the simulation are compared with continuously measured glucose data. Figure E.3 shows the predicted glucose concentrations (bold line) against ±1SD (n=11) confidence limits (grey area) of the CGMS trace. Our results are within the ±1SD confidence limits of continuously measured signals (measured in 11 healthy persons.

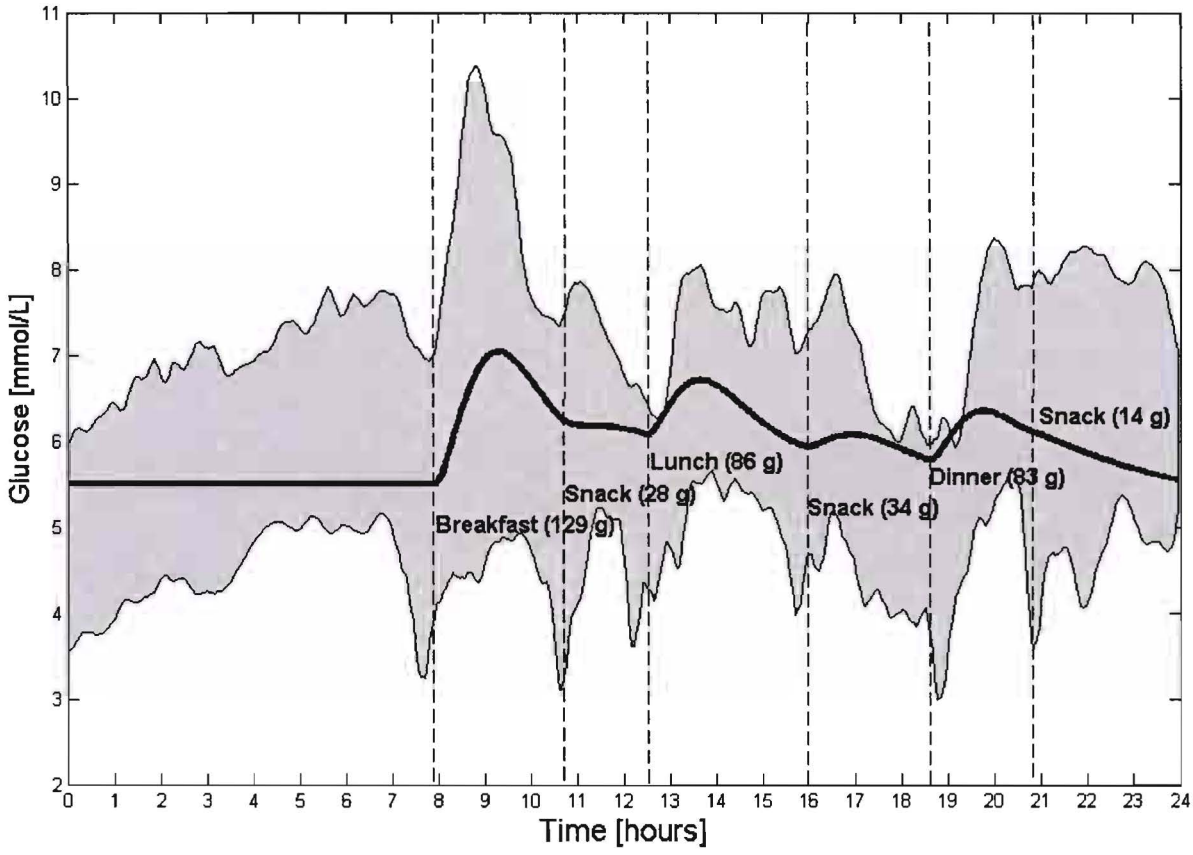

Figure E.3: Predicted glucose concentrations (bold line) versus measurement of glucose concentrations (± 1SD CGMS, grey area) in a healthy person.

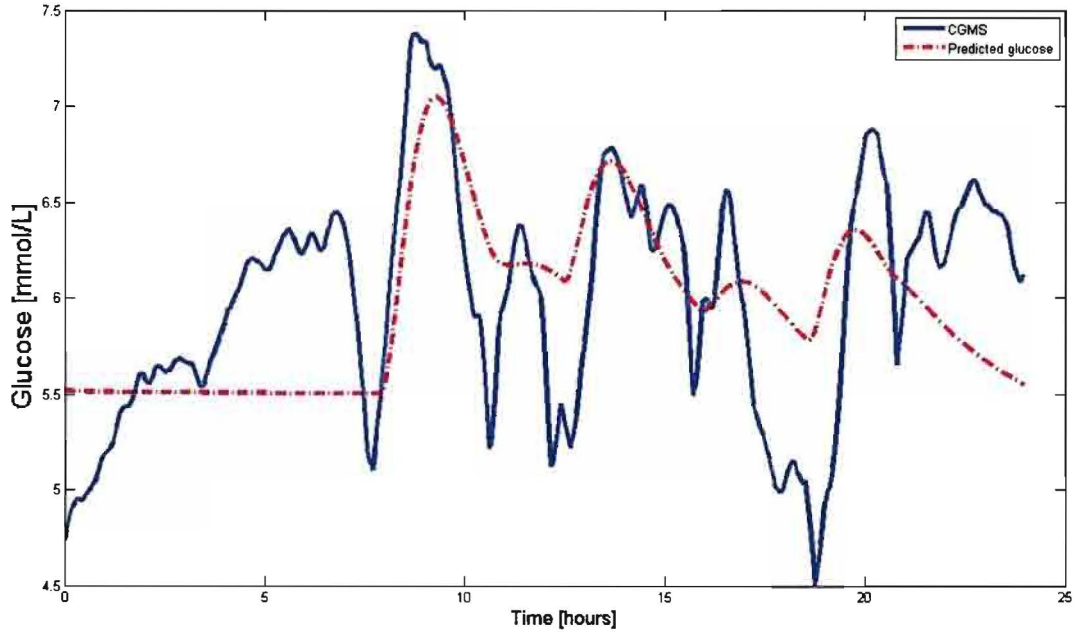

Figure E.4: Predicted glucose concentrations (dashed line) using estimated parameters versus averaged (11 subjects) measured glucose trace.

b. Results for a type-1 diabetes patient without exogenous insulin

In order to simulate a type-1 diabetes patient, the pancreas (PID-model) function was decreased to 50% and 10%. The decrease in pancreas function represents the different stages of the severity of the disease. The remaining model parameters were assumed to be unchanged in a type-1 diabetes patient and there was no exogenous insulin injected.

Figure E.5 shows the predicted glucose and insulin concentration of a 70 kg type-1 diabetes subject before and after the consumption of 75 g glucose. Glucose was orally ingested at t=0 min. The plasma and delivered insulin concentration decrease while the pancreas function decreases from 100% to 10%. Next to that, the first phase response (first peak) of the pancreas disappears with the decrease of pancreas function. The plasma glucose trace of figure E.5 shows that the concentration of glucose is higher in a diabetic patient with 10% pancreas function than in a healthy person (100% pancreas function), difference of approximately 1 mmol/L, and that it takes more than 24 hours for the plasma glucose concentration of a type-1 diabetic patient (10% pancreas function) to return to its basal value. The glucose concentration in the gut is not affected by the pancreas function.

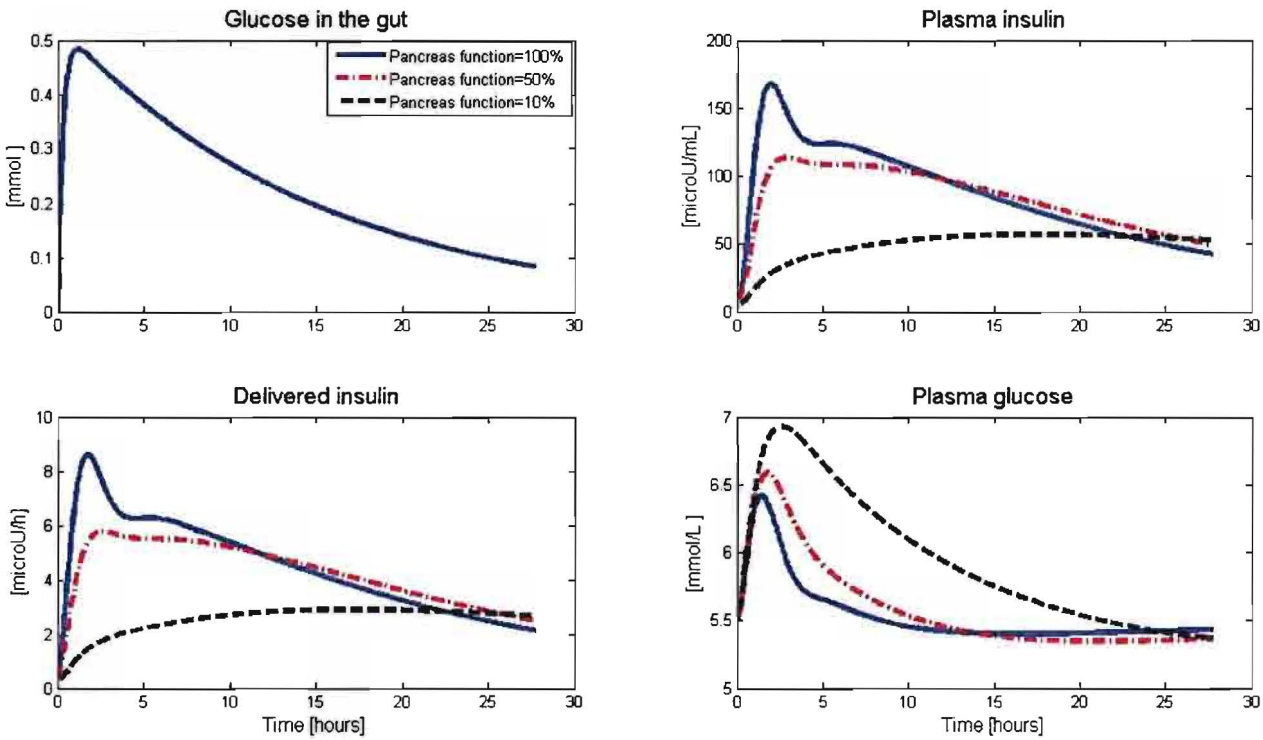

Figure E.5: Predicted glucose and insulin concentration time-courses for a 70 kg type-1 diabetes patient. Glucose (75 g) was orally ingested at t=0 min and there was no exogenous insulin injected.

c. Results for a type-1 diabetes patient with exogenous insulin

The model was also used to simulate a type-1 diabetes patient that uses insulin, by injecting 3 units of insulin (Regular) and assuming a pancreas function of 10%. The remaining models parameters were assumed unchanged. Figure E.6 shows the predicted plasma glucose concentrations of a type-1 diabetes patient (solid line) versus the predicted plasma glucose concentrations (dashed line) of a healthy person. The figure shows that the plasma glucose trace in the type-1 diabetes patient reaches its maximum 180 minutes later than the healthy person. Furthermore, it takes more than 24 hours for the diabetic glucose trace to return to its basal value, whereas the healthy one returns within 5 hours to its basal value.

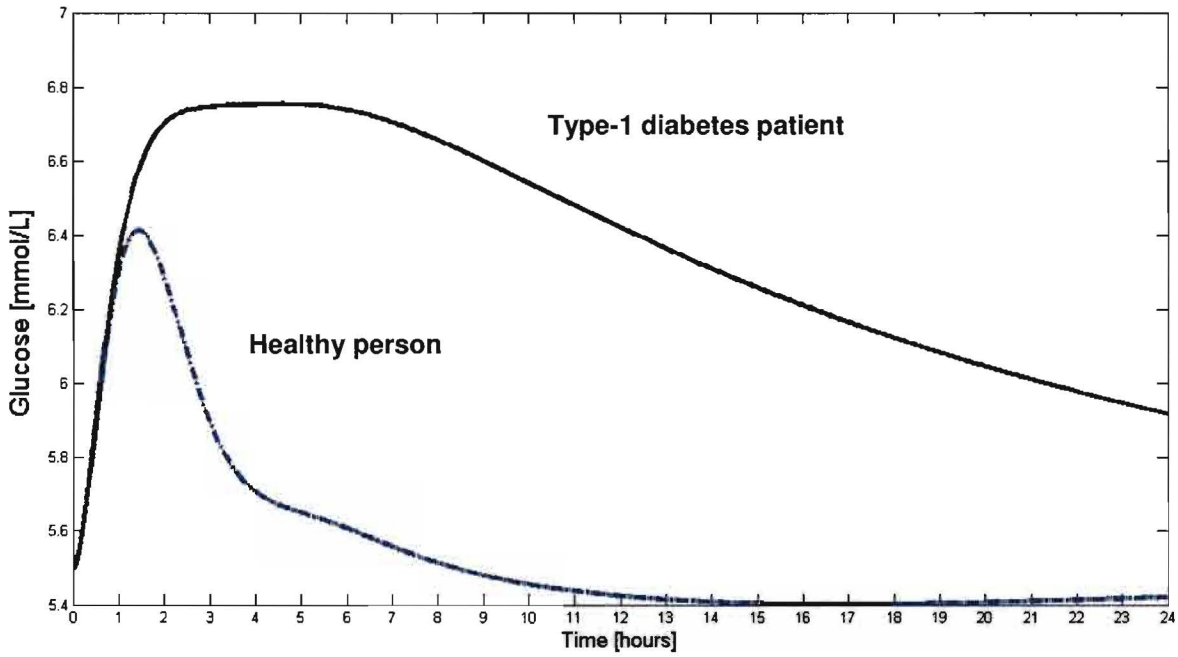

Figure E.6: Predicted glucose concentrations of a type-1 diabetes patient (carbohydrate consumption=75 g at t=0 min; insulin injection=3 units Regular at t=0 min)

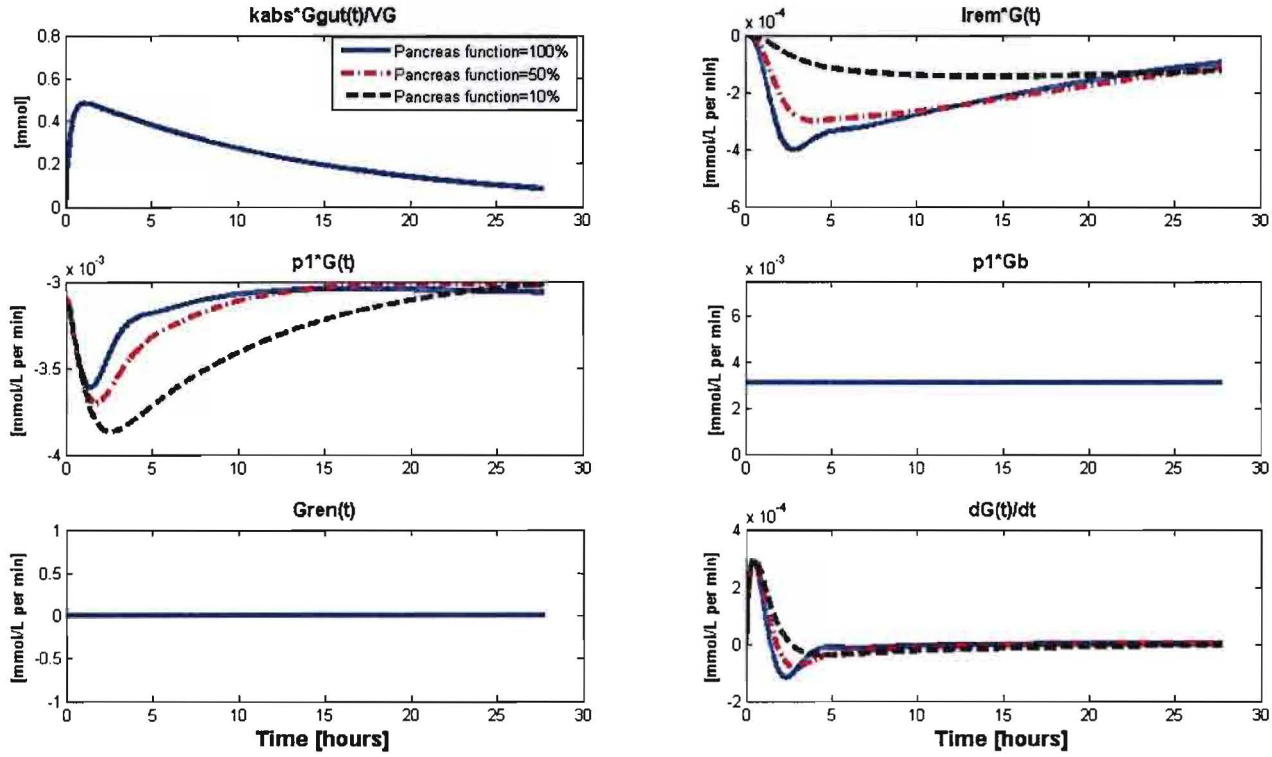

*Figure E.7: Endogenous glucose production (kabs*Ggut(t)/V_G and p1*G(t)), insulin-dependent (Irem*G(t)), insulin-independent glucose utilization (p1*G(t)), renal excretion (Gren(t)) and the plasma glucose change in time (dG/dt)*

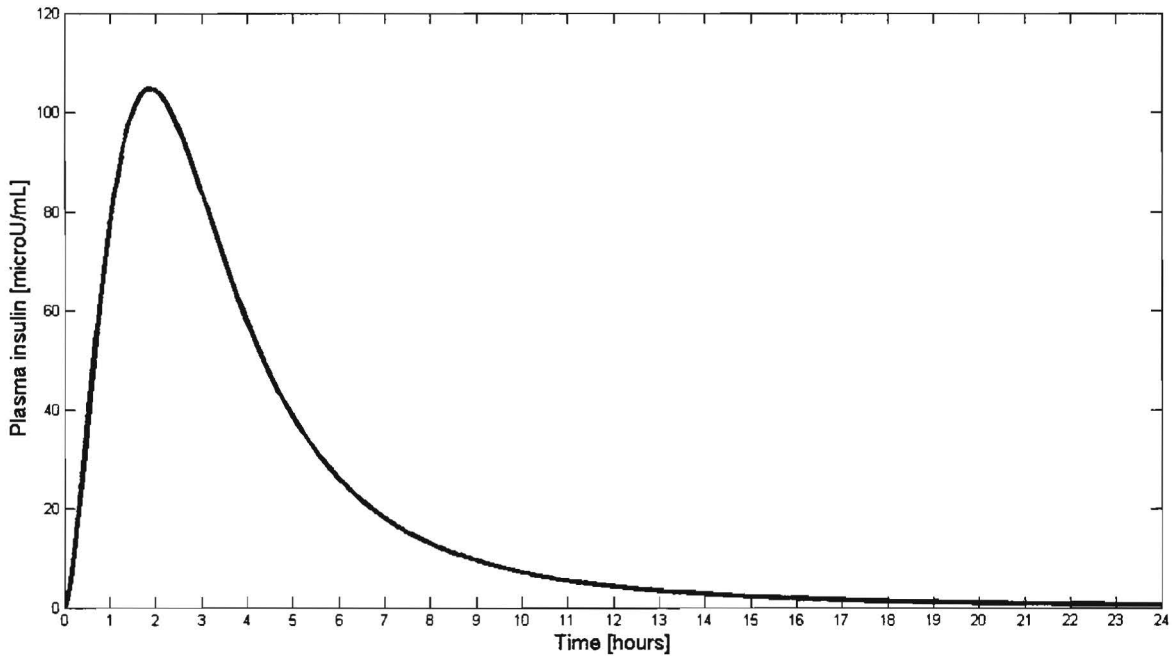

Figure E.8: A predicted time course of absorption for insulin (Regular) after subcutaneous injection of 24 units.

3. Discussion

The results of the simulation for a healthy subject using parameters from the literature show that the predicted plasma glucose and rate of glucose appearance are within the physiological range. This is not the case for plasma insulin, where the concentration is three times as large as the normal value and the time to peak concentration is about three times faster than values reported in vivo. From this, we can report that the delivered insulin is also not within the physiological range, even if our results are comparable to the results of Steil *et al.* [16]. The cause of the high concentration and fast increase of plasma insulin may be the cause of high delivery rates of insulin by the β-cell. Furthermore, the model of Steil *et al.* is not validated against measured data. The graph, shown in figure B.3, that we used to evaluate our results, is theoretical. We looked at simulated results of Steil *et al.*, but as they use the PID-model for another purpose (development of a closed-loop system), these data were not useful to compare our results to. However, when we looked at their simulations obtained by using a measured glucose data as input, we observed that they do not achieve to obtain results comparable to the graph shown in figure 1.

In order to improve the performance of the model, we estimated the model parameters using continuously measured glucose data (CGMS data). The results of a multiple meal simulation using the estimated parameters (figure E.3) show that the plasma glucose predicted by our model is within the ±1SD confidence limits of the measured glucose trace. Furthermore, the plasma insulin concentration is approximately within the physiological range of healthy subjects (150 μU/mL). We cannot comment on the rate of glucose appearance and the delivered insulin concentration because we don't have measured data of these concentrations.

Figure 6 shows the average (11 subjects) measured glucose concentrations against the predicted glucose trace using the estimated parameters. This figure shows that there is still a difference between the measured and predicted glucose concentration. These differences may be caused by different factors, which will be explained here. During the nocturnal fasting period (0-8 hours in figure E.3), the plasma glucose concentration predicted by our model is constant (around 5.5 mmol/L). This is not the case for the measured glucose concentration. This shows that our model lacks some metabolic processes such as those that occur during the night fasting, see appendix A. This may be one of the causes of the differences between the predicted glucose trace and the measured one. Next to that, our model

does not take movement, emotions and other regulatory hormones than insulin (such as the counter regulatory hormone glucagon) into account. Furthermore, during the measurement of the glucose trace (CGMS), the subjects had a complex meal that contains, next to carbohydrate, protein and fat. Our model only uses a carbohydrate-rich meal as food intake. In addition, the measured CGMS data were from persons that were age and BMI-matched to a diabetes group [20]. Consequently, these subjects have a relatively high BMI (average: 27.8). As a high BMI is related to insulin resistance, we are wondering how healthy this patient group is. The large variability in glucose concentrations among the subjects and relatively high glucose concentrations (up to 16 mmol/L) during the day in the data confirms this. This variability also makes it difficult to estimate the model parameters accurately.

We also used our model to simulate a type-1 diabetes patient that uses insulin. The time course of absorbed insulin is shown in figure E.8. The plasma insulin trace is identical to that reported by Berger [10]. For the sake of comparison with Berger, we simulated an injection of 24 units. The results of the simulation (10% pancreas function, 3 units injection of Regular insulin, 75 g carbohydrate consumption in a 70 kg person) show that the plasma glucose trace in the type-1 diabetes patient reaches its maximum 180 minutes later than the healthy person and that the plasma glucose concentration is not returned to its basal value before 24 hours (5 hours in a healthy person). This may occur in type-1 diabetes patients. At the moment, we don't have measured data of type-1 diabetes patients to evaluate this. Our results show also that the type and dose of insulin used during this simulation is not suitable because we didn't achieve a good glycaemic control (glucose concentration didn't not return to its basal value within 5 hours as occurs in healthy persons), which is the aim of insulin therapy. More insulin types should be therefore added to the model.

Using the new estimated parameters, we also investigated the influence of the decrease of pancreas function, in absence of subcutaneous insulin injection, on the plasma glucose. The results show that when the pancreas function is decreased from 100% to 10%, the predicted plasma glucose remains within the normal physiological range. In type-1 diabetes patient where the pancreas does not produce insulin and where no exogenous insulin is injected, the plasma glucose increases to a higher value. The relatively low plasma glucose concentration in our model may

be caused by assuming the remaining parameters equal to the parameters of a healthy person. Dalla Man *et al.* [21]showed in their study that there is a difference between model parameters for healthy and diabetes subjects.

In order to find out why the plasma glucose concentration decreases in absence of insulin, the endogenous glucose production, the insulin-dependent and insulin-independent glucose utilization, renal excretion and the plasma glucose change in time were plotted, see figure E.7. This figure shows that when the pancreas function decreases and the insulin-dependent utilization consequently decreases, the insulin-independent utilization increases. This occurs because the minimal model of Bergman assumes a linear relationship between the rate of insulin-independent glucose utilization (p_1) and plasma glucose concentration (G) that increases due to the absence of insulin. The product of G and p_1, which represents the insulin-independent utilization, increases with the increase of glucose concentration. There is a recent published study [21] where a Michaelis-Menten relationship is used instead of a linear one. This may be more suitable for our model too.

4. Conclusion

In conclusion, we showed that our glucose-insulin model achieved to predict glucose concentrations in healthy persons, within (qualitatively) acceptable accuracy for education purposes. However, the glucose-insulin for healthy persons should be validated against another dataset. During this study, we used the same dataset for parameter estimation as for the (qualitative) validation.

The predictions in type-1 diabetic patients did not result in realistic prediction of glucose concentrations. This may be caused by using model parameters for healthy subjects. During the simulation of a type-1 diabetes patient, we only decreased the pancreas β-cell function, which represents a type-1 diabetes patient that lacks insulin production, while the remaining parameters were unchanged.

The results of the simulations should be validated quantitatively. For this purpose, we should quantitatively define the acceptable accuracy of our model prediction. We may use a Clarke Error Grid for this goal. This grid is usually used to quantify the accuracy of blood glucose meters as compared to a reference value. "The grid

breaks down a scatter plot of a reference glucose meter and an evaluated glucose meter into five regions. Region A are those values within 20% of the reference sensor, Region B contains points that are outside of 20% but would not lead to inappropriate treatment, Region C are those points leading to unnecessary treatment, Region D are those points indicating a potentially dangerous failure to detect hypo- or hyperglycemia, and Region E are those points that would confuse treatment of hypoglycemia for hyperglycemia and vice-versa" [22]. As our model will be used for educational purposes, it is not highly required to have an accurate model. However, how accurate is accurate enough for educational purposes?

Appendix F: Parameter estimation using CGMS data

This document describes parameter estimation of the glucose-insulin model described in appendix B.

1. Model equations

The differential equations that describe the model are given below:

$$\frac{dG_{gut}(t)}{dt} = D_G k \beta e^{(-kt)^{\beta}} - k_{abs} G_{gut}(t) \qquad G_{gut}(t_0) = G_{gut0}$$

$$\frac{dG}{dt} = -p_1 G(t) - I_{rem}(t) G(t) + p_1 G_b + \frac{k_{abs} G_{gut}}{V_G} - \frac{G_{ren}}{V_G} \qquad G(t_0) = G_0$$

$$\frac{dI_{rem}}{dt} = -p_2 I_{rem}(t) + p_3 \left(I_p(t) - I_b\right) \qquad I_{rem}(t_0) = I_{rem0}$$

$$\frac{dI_p}{dt} = p_5 I_D(t) - \mathrm{k_e} I_p(t) \qquad I_p(t_0) = I_{p_0}$$

Where:

$$I_D(t) = K_p \left(G(t) - \mathrm{G_B}\right) + \frac{K_P}{T_I} \int \left(G(t) - G_B\right) dt + K_p T_D \frac{dG(t)}{dt} \qquad I_D(t) \geq 0$$

2. CGMS data

The parameters were estimated using 17 hour (325 sample points) Continuous Glucose Monitoring System (CGMS) data. These data were measured from 11 healthy normoglycaemic subjects (Age=59 ± 2 years; BMI=27.8 ± 1.4 kg/m^2). The subjects took standardized meals [43.8 kJ/kg of body weight, consisting of 60 En% (energy %) carbohydrate, 28 En% fat and 12 En% protein]. The meal and beverages were provided in pre-weighed packages and ingested at pre-determined time points to ensure fully standardized dietary modulation. During the measurement period, subjects received a standardized diet (three meals and three snacks per day). Whenever the subjects deviated from the prescribed diet-scheme, they reported this to the investigators.

More information about the measurement procedure and the subjects is given in [20]. The subjects received different meals, containing carbohydrate, protein and fat, during the day. The amount of carbohydrate and the time of food intake per subject is given in table F.1 and table F.2 respectively.

Table F.1: Amount of carbohydrate (grams) ingested during the day

Meal	1	2	3	4	5	6	7	8	9	10	11	AVG	SD
Breakfast	113	143	143	143	113	113	143	143	143	143	83	129.4	19.7
Snack	28	28	28	28	28	28	28	28	28	28	28	28.0	0
Lunch	80	80	110	110	80	80	80	110	80	80	60	86.4	15.5
Snack	34	34	34	34	34	34	34	34	34	34	34	34.0	0
Diner	83	83	83	83	83	83	83	83	83	83	83	83.0	0
Snack	14	14	14	14	14	14	14	14	14	14	14	14.0	0

Table F.2: Time of food intake during the day

Meal	1	2	3	4	5	6	7	8	9	10	11	AVG	SD
Breakfast	7:40	7:50	7:30	7:30	8:00	9:10	8:30	7:40	7:30	7:40	7:30	7:51	0:31
Snack	10:30	10:30	10:30	10:30	10:05	11:30	11:00	10:40	10:30	10:30	10:30	10:36	0:21
Lunch	12:10	12:30	12:00	12:00	12:00	13:30	13:00	12:30	13:00	12:00	12:15	12:26	0:30
Snack	15:15	16:00	15:30	15:30	17:00	16:10	16:30	15:30	16:00	15:30	15:30	15:51	0:32
Diner	18:30	18:45	18:30	18:30	18:30	18:30	18:30	18:40	18:30	18:30	18:30	18:32	0:05
Snack	20:30	20:30	20:30	20:30	19:30	20:30	20:30	20:30	20:30	20:30	20:30	20:24	0:18

3. Parameter estimation

Using an average trace of the 11 subjects (as output) and the average values for food consumption (as input), we estimated all the parameters given in table F.3, except $p_5=1/V_I$, V_G, G_{FR}, R_{TG}, I_b and G_b. The reason for excluding these parameters is that we assume that they are well estimated in the literature. The Parameter Estimation toolbox of Simulink® was used to perform the estimation. Table F.3 shows the initial parameters taken from the literature. The estimated parameters are shown in table F.4.

Table F.3: Initial model parameters from the literature

Parameter	Value	Unit
p_1	$3.38 \cdot 10^{-2}$	[1/min]
p_2	$2.09 \cdot 10^{-2}$	[1/min]
p_3	$7.51 \cdot 10^{-6}$	[ml/μU/min²]
p_5	$p_5=1/V_I$	[1/ml]
K_p	$0.2 \cdot 10^6$ [μU/min per mmol/l]	[μU/min per mmol/l]
T_I	100	[min]
T_D	40	[min]
I_{DB}	0	[μU/min]
D_G	Carbohydrate intake	[mmol]
k_{abs}	$2.89 \cdot 10^{-2}$	[1/min]
k	0.014	[1/min]
β	1.23	dimensionless
V_G	0.17 x 70	[l]
V_I	$0.142 \cdot 10^3$ x 70	[ml]
k_e	0.09	[1/min]
G_{FR}	100 ml/min	[ml/min]
R_{TG}	9 mmol/l	[mmol/l]

Table F.4: Estimated model parameters

Parameter	Initial	Estimated	Unit
Kp	200000	114060	μU/min per mmol/L
Td	40.0	0,003	min
Ti	100.0	199,95	min
beta	1.23	0,32	dimensionless
k	0.0140	0,0035	1/min
kabs	0.029	0,058	1/min
ke	0.090	0,085	1/min
p1	0.034	0,016	1/min
p2	0.021	0,019	1/min
p3	$7.5 \cdot 10^{-6}$	$0,57 \cdot 10^{-6}$	ml/μU/min²

4. Discussion

Figure E.3 shows a 24 h predicted glucose concentrations (bold line) against ±1SD (n=11) confidence limits (grey area) of the CGMS trace used during the estimation. This figure shows that during the nocturnal fasting period (0-8 hours in figure E.3), the plasma glucose concentration predicted by our model is constant (around 5.5 mmol/L). This is not the case for the measured glucose concentration. This shows that our model lacks some metabolic processes such as those that occurs during the night fasting. This may be one of the causes of the differences between the predicted glucose trace and the measured one. Next to that, our model does not take movement, emotions and other regulatory hormones than insulin (such as the counter regulatory hormone glucagon) into account. Furthermore, during the measurement of the glucose trace (CGMS), the subjects had a complex meal that contains, next to carbohydrate, protein and fat. Our model only takes carbohydrate ingestion into account. In addition we used the average CGMS trace and the average food intake during to estimate the parameters. As these values were not constant for all the subjects, the results of the estimation may be affected by this. We tried to estimate the parameters per subject but this did not give better results because of the large variability in glucose concentration among the subjects.

Appendix G: The user interface of the simulator

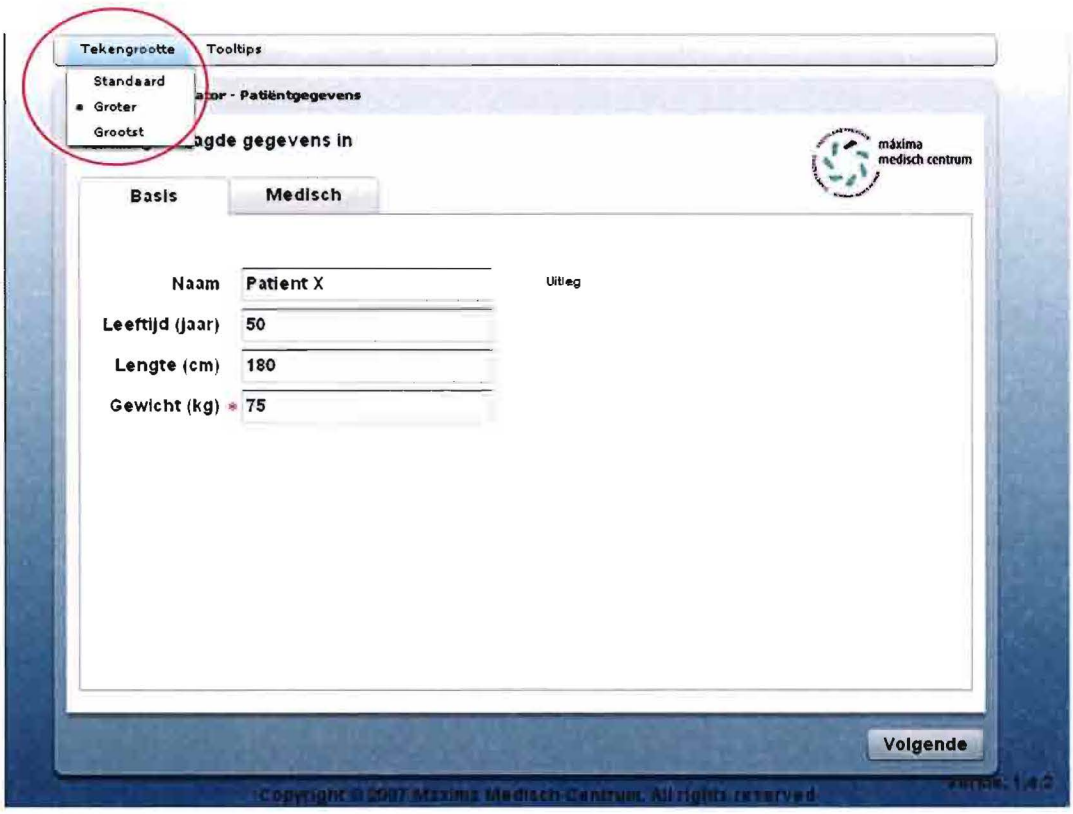

Figure G.1: Patient categorization page (basic)

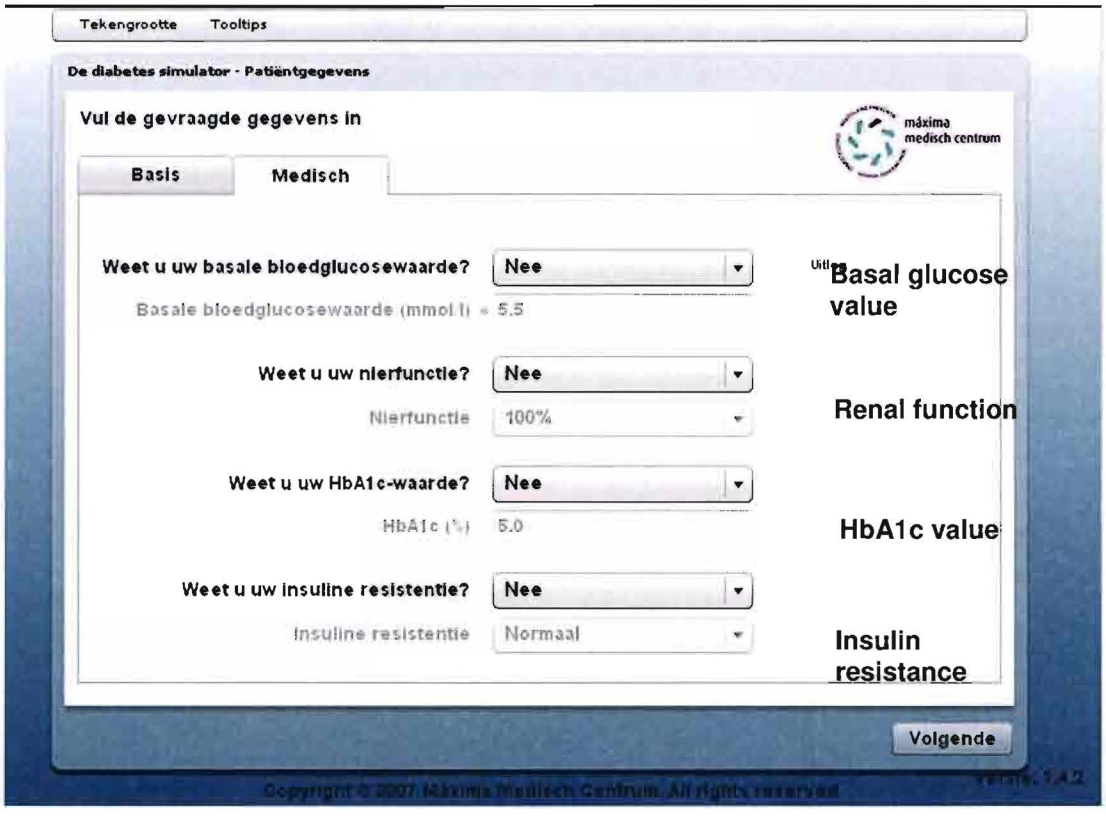

Figure G.2: Patient categorization page (medical)

Figure G.3: Selection of one of the three levels

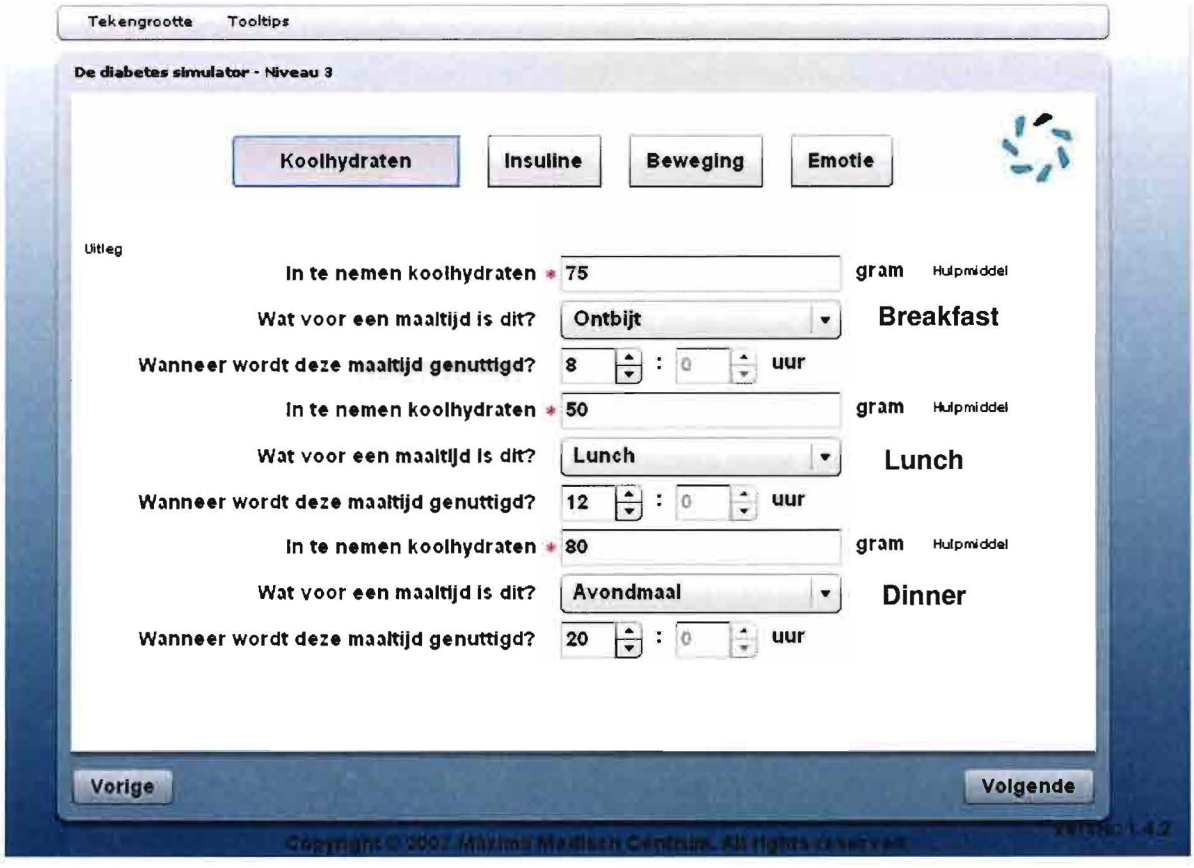

Figure G.4: Carbohydrate intake for three different meals

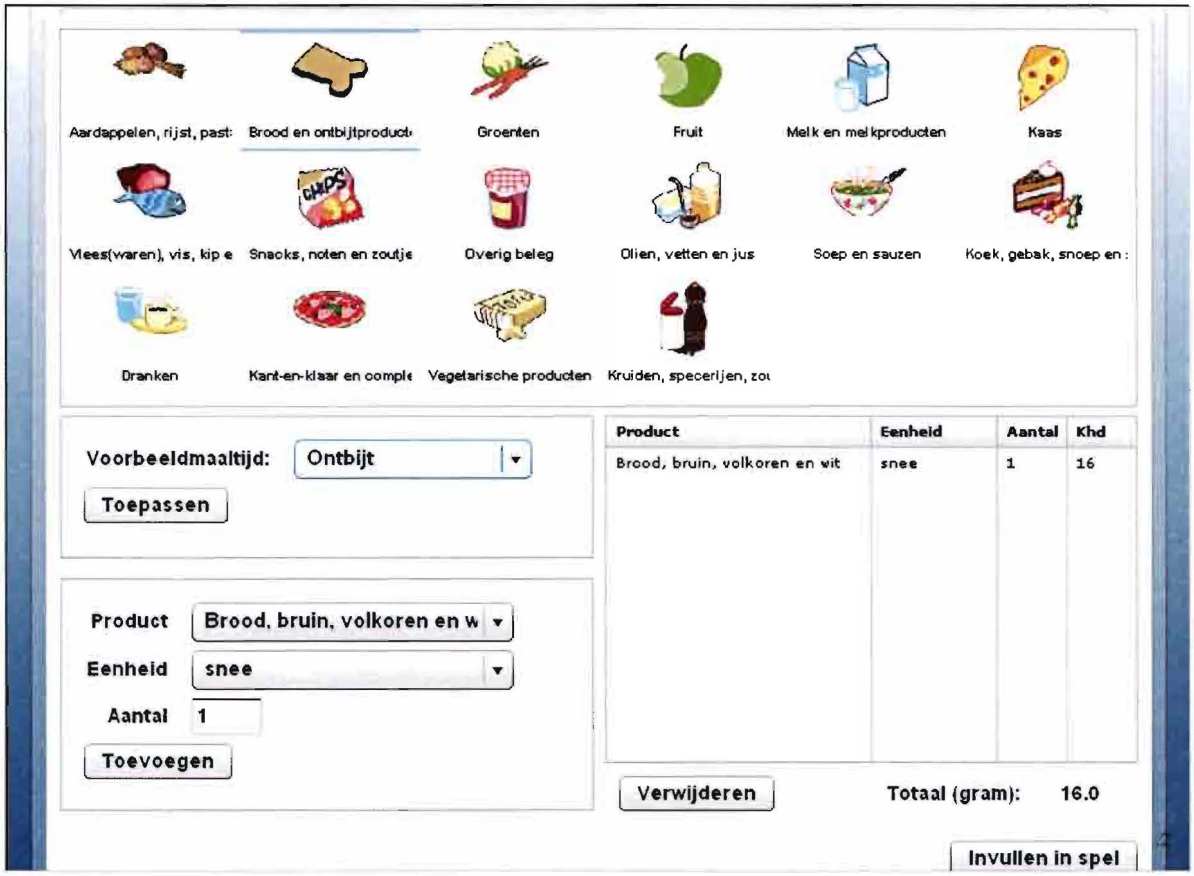

Figure G.5: The carbohydrate calculator

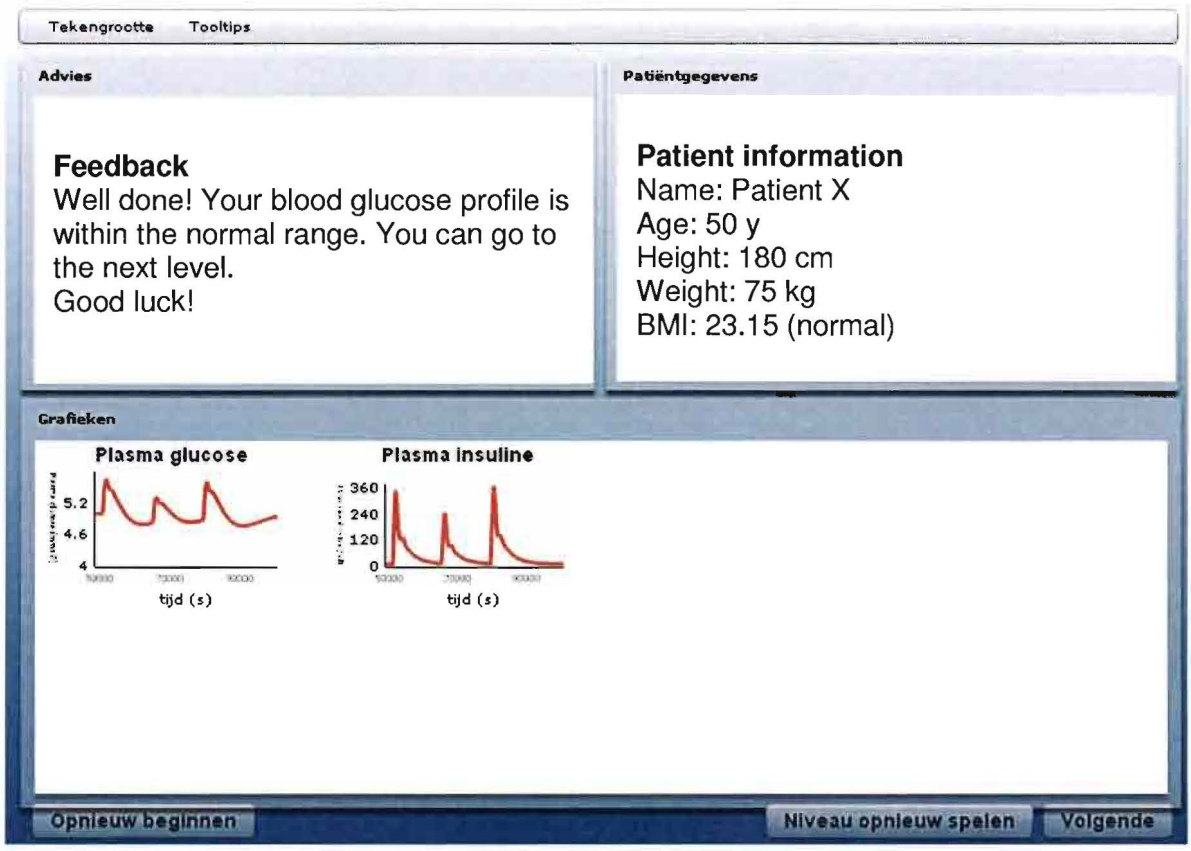

Figure G.6: Results of the simulation and feedback

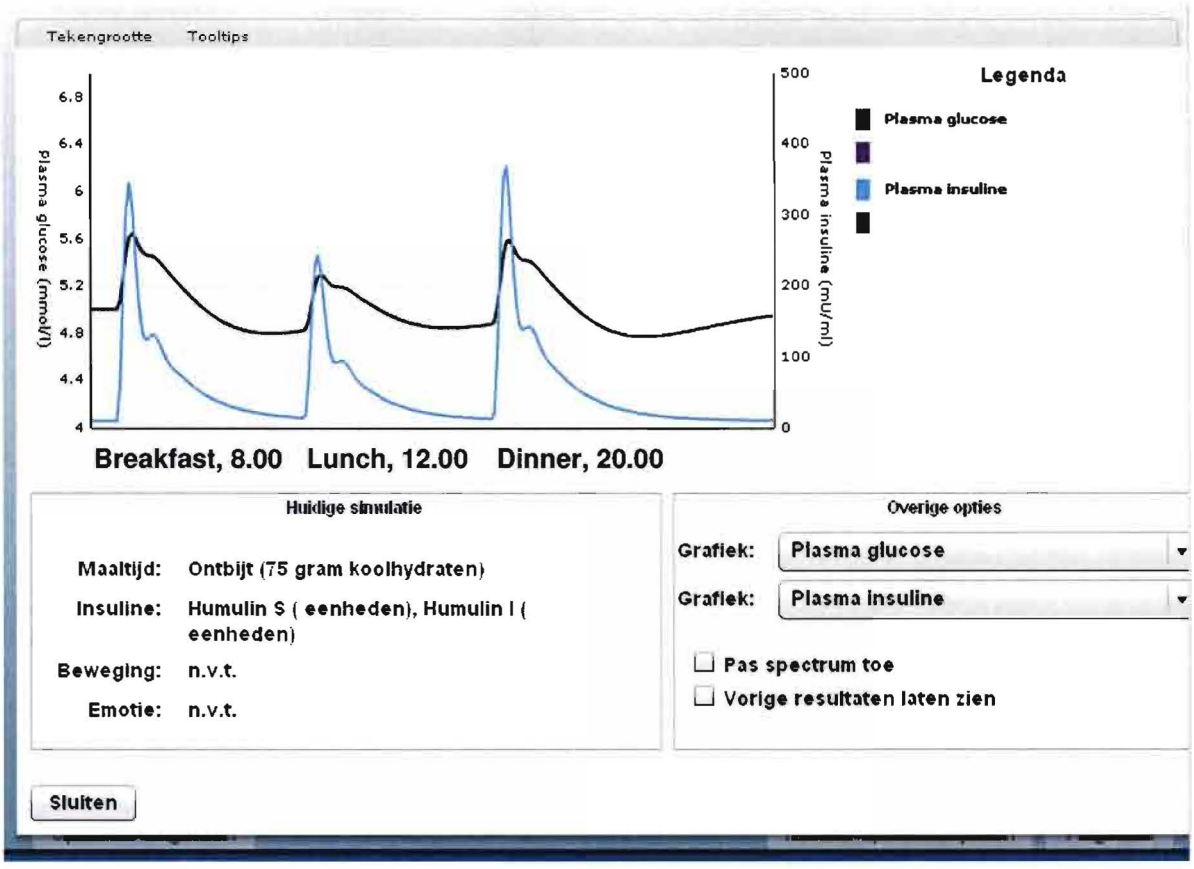

Figure G.7: Plasma glucose and insulin in the same graph

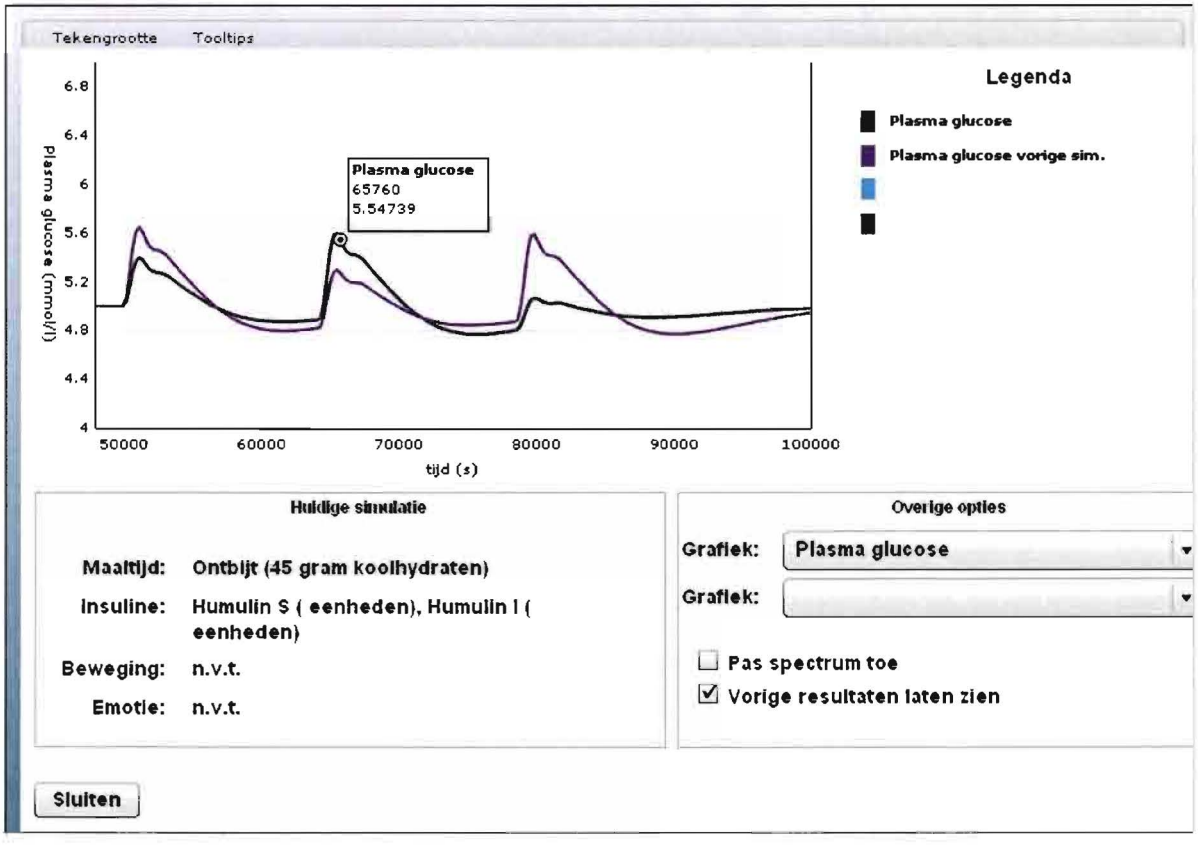

Figure G.8: The previous and current simulation results for plasma glucose in the same graph

Bibliography

[1] http://www.who.int/diabetes/facts/en/

[2] *Diabetes Atlas*, 2nd ed. Brussels: International diabetes foundation, 2003.

[3] *Textbook of Diabetes*, 2nd ed. Oxford: Blackwell Science, 1997.

[4] F.S.Greenspan and D.G.Gardner, *Basic & Clinical Endocrinology*, 7th ed McGraw Hill Companies, Inc., 2004.

[5] P.E.Molina, *Endocrine Physiology*, 2nd ed. New York: McGraw-Hill Companies, Inc., 2006.

[6] R. N. Bergman, Y. Z. Ider, C. R. Bowden, and C. Cobelli, "Quantitative estimation of insulin sensitivity," *Am. J Physiol*, vol. 236, no. 6, p. E667-E677, June1979.

[7] G. M. Steil, K. Rebrin, R. Janowski, C. Darwin, and M. F. Saad, "Modeling beta-cell insulin secretion--implications for closed-loop glucose homeostasis," *Diabetes Technol Ther.*, vol. 5, no. 6, pp. 953-964, 2003.

[8] S. Natalucci, F. Di Nardo, P. Staffolani, C. De Marzi, P. Morosini, and R. Burattini, "Glucose absorption and insulin sensitivity from oral glucose tolerance test," *Engineering in Medicine and Biology Society, 2003. Proceedings of the 25th Annual International Conference of the IEEE*, vol. 3, pp. 2758-2760, 2003.

[9] E. D. Lehmann and T. Deutsch, "A physiological model of glucose-insulin interaction in type 1 diabetes mellitus," *J Biomed. Eng*, vol. 14, no. 3, pp. 235-242, May1992.

[10] M. Berger and D. Rodbard, "Computer simulation of plasma insulin and glucose dynamics after subcutaneous insulin injection," *Diabetes Care*, vol. 12, no. 10, pp. 725-736, Nov.1989.

[11] R. N. Bergman, D. T. Finegood, and M. Ader, "Assessment of insulin sensitivity in vivo," *Endocr. Rev.*, vol. 6, no. 1, pp. 45-86, 1985.

[12] J. E. Gerich, "Is reduced first-phase insulin release the earliest detectable abnormality in individuals destined to develop type 2 diabetes?," *Diabetes*, vol. 51 Suppl 1, p. S117-S121, Feb.2002.

[13] R. E. Pratley, J. E. Foley, and B. E. Dunning, "Rapid acting insulinotropic agents: restoration of early insulin secretion as a physiologic approach to improve glucose control," *Curr. Pharm. Des*, vol. 7, no. 14, pp. 1375-1397, Sept.2001.

[14] C. J. De Souza, K. Gagen, W. Chen, and N. Dragonas, "Early insulin release effectively improves glucose tolerance: studies in two rodent models of type 2 diabetes mellitus," *Diabetes Obes. Metab*, vol. 3, no. 2, pp. 85-95, Apr.2001.

[15] G. M. Steil, A. E. Panteleon, and K. Rebrin, "Closed-loop insulin delivery-the path to physiological glucose control," *Adv. Drug Deliv. Rev.*, vol. 56, no. 2, pp. 125-144, Feb.2004.

[16] G. M. Steil, K. Rebrin, C. Darwin, F. Hariri, and M. F. Saad, "Feasibility of automating insulin delivery for the treatment of type 1 diabetes," *Diabetes*, vol. 55, no. 12, pp. 3344-3350, Dec.2006.

[17] R. N. Bergman, L. S. Phillips, and C. Cobelli, "Physiologic evaluation of factors controlling glucose tolerance in man: measurement of insulin sensitivity and beta-cell glucose sensitivity from the response to intravenous glucose," *J Clin Invest*, vol. 68, no. 6, pp. 1456-1467, Dec.1981.

[18] J. Schirra, M. Katschinski, C. Weidmann, T. Schafer, U. Wank, R. Arnold, and B. Goke, "Gastric emptying and release of incretin hormones after glucose ingestion in humans," *J Clin Invest*, vol. 97, no. 1, pp. 92-103, Jan.1996.

[19] A. E. Panteleon, M. Loutseiko, G. M. Steil, and K. Rebrin, "Evaluation of the effect of gain on the meal response of an automated closed-loop insulin delivery system," *Diabetes*, vol. 55, no. 7, pp. 1995-2000, July2006.

[20] S. F. Praet, R. J. Manders, R. C. Meex, A. G. Lieverse, C. D. Stehouwer, H. Kuipers, H. A. Keizer, and L. J. van Loon, "Glycaemic instability is an underestimated problem in Type II diabetes," *Clin Sci. (Lond)*, vol. 111, no. 2, pp. 119-126, Aug.2006.

[21] M. C. Dalla, R. A. Rizza, and C. Cobelli, "Meal simulation model of the glucose-insulin system," *IEEE Trans. Biomed. Eng*, vol. 54, no. 10, pp. 1740-1749, Oct.2007.

[22] http://*www.wikipedia.com*